Chapter IV: Results and discussion: $[Cr_3O(F_3CCO_2)_6.3H_2O]NO_3.H_2O$ as Ziegler-Natta catalyst for ethylene polymerization

4.1 Introduction

The synthesis of $[Cr_3O(F_3CCO_2)_6.3H_2O]NO_3.H_2O$, polymerization procedure and polymer characterization method were discussed in full in chapters 2 and 3. The trinuclear oxo-centered chromium complex of $[Cr_3O(F_3CCO_2)_6.3H_2O]NO_3.H_2O$ (15.85% of Cr content) is stable at ambient temperature. In addition, it was ground to powder prior to using it for polymerization experiments.

The reactor used for the polymerization experiments, was a 1000 mL autoclave Parr reactor. All experiments were run using about 0.08 g of chromium complex. The total volume of polymerization solution was 400 mL and the polymerization temperature was constant at 40 ^oC unless otherwise stated. The temperature was maintained by adding ice occasionally in the water bath.

This present chapter describes the use of $[Cr_3O(F_3CCO_2)_6.3H_2O]NO_3.H_2O$, in combination of $AlEt_2Cl$ as a heterogeneous Ziegler-Natta catalyst system for ethylene polymerization. This catalytic system, with toluene as medium, was initially green in color but turned yellow after one minute of ageing time. The change in color may indicate the formation of new complex between the chromium(III) complex and the $AlEt_2Cl$. According to previous literature [1-3], describing studies of similar types of complexes, the valence state of the chromium has been changed from III to II.

Some unique effects of different initial monomer pressures and Cr / Al ratios on the rate of the polymerization and catalytic activity under similar conditions were observed. They are summarized in the following sections.

4.2 Kinetics of ethylene polymerization

Kinetic data are of great importance because they can help estimate the rate law, number of polymerization centers, activation energy and the average lifetime of the growing polymer chains.

Many kinetic schemes for heterogeneous Ziegler-Natta polymerization have been proposed in review articles over the years [4-6], but they are complicated and frequently difficult to confirm experimentally [7].

Under ethylene polymerization conditions of constant volume (V) and temperature (T), the total monomer pressure (P) is directly proportional to the number of moles (n) of ethylene in the mixture as:

$$P = \frac{nRT}{V} \qquad \text{IV-1}$$

where R = gas constant

In this work, kinetics of the polymerization of ethylene in the presence of trinuclear oxo-centered chromium(III) carboxylate complexes were investigated by monitoring the drop in monomer pressure against time. The polymerization reaction can be represented by the equation:

$$n\,CH_2{=}CH_2 + \text{Cr(III) complex / } AlEt_2Cl \longrightarrow -\left(CH_2\text{-}CH_2\right)_n- \qquad \text{IV-2}$$

Assuming the reaction is a first order reaction, the rate of the reaction is given by the equation:

$$\frac{-dC}{dt} = kC \qquad \text{IV-3}$$

where k = overall rate constant for the polymerization reaction

Assuming the pressure in a closed system (autoclave reactor) is proportional to the molar monomer concentration (C), thus equation IV-1 can be written as:

$$P = CRT \qquad (C = n/V) \qquad \text{IV-4}$$

Thus the rate of change of pressure as a function of time would be:

$$\frac{dP}{dt} = \frac{d(CRT)}{dt} = RT\frac{dC}{dt} \qquad \text{IV-5}$$

By substituting equation IV-3 into IV-5, we obtain

$$\frac{dP}{dt} = -kCRT = -kP \qquad \text{IV-6}$$

Thus,

$$\frac{dP}{P} = -kdt \qquad \text{IV-7}$$

By integrating equation IV-7 we obtain

$$\int(dP/P) = -k\int dt$$

Thus,

$$\ln P = -kt + c$$

Where k represents the overall rate constant of the polymerization, P the pressure of ethylene at time (t). Thus a plot of ln P versus time should give a straight line.

A typical set of experimental data to verify the first order reaction is given in Table 4.1. The first column indicates the time of the reaction in minutes. Column two shows the ethylene pressure at different reaction times. An initial ethylene pressure of 913 kPa is used. The amount of ethylene that has reacted after time (t) is expressed in mol and shown in column five. This value was calculated using $\Delta n = \Delta P(V/RT)$. Δn is the number of moles of monomer reacted while ΔP represents the drop in pressure due to ethylene consumed at that particular time (column four). The volume of ethylene gas (V) is given as $V_R - V_S$, where V_R is the total volume of the reactor and V_S is the volume of the reaction solution. The temperature is expressed in Kelvin, volume is in dm^{-3}, the pressure in kPa and R equals to 8.314 $Jmol^{-1}K^{-1}$.

Table 4.1: Kinetic data of a typical polymerization reaction

Time (min)	C_2H_4 Pressure, P (kPa)	ln P	Drop of C_2H_4 Pressure, ΔP (KPa)	C_2H_4 Reacted, Δn (mol)	Catalytic activity (g-PE/g-Cr/hr/atm)
0	913	6.8167	0	0	0
0.5	900	6.8024	13	0.00338	3765.15
1	877	6.7765	23	0.00598	6491.18
1.5	863	6.7604	14	0.00364	3888.08
2	845	6.7393	18	0.00468	4894.69
2.5	837	6.7298	8	0.00208	2154.82
3	827	6.7178	10	0.0026	2661.35
3.5	818	6.7069	9	0.00234	2369.15
4	810	6.697	8	0.00208	2085.31
4.5	803	6.6884	7	0.00182	1808.88
5	785	6.6657	18	0.00468	4547.14
5.5	775	6.6529	10	0.0026	2494.01
6	768	6.6438	7	0.00182	1730.04
7	760	6.6333	8	0.00208	1956.59
7.5	755	6.6267	5	0.0013	1214.82
9	745	6.6134	10	0.0026	2397.47
10	742	6.6093	3	0.00078	716.344
11	733	6.5971	2	0.00052	471.77
12	723	6.5834	10	0.0026	2326.67
13	695	6.5439	17	0.00442	3802.16
14	688	6.5338	7	0.00182	1549.83
15	683	6.5265	2	0.00052	439.589
16	680	6.5221	3	0.00078	656.488
17	677	6.5177	3	0.00078	653.591
18	673	6.5117	4	0.00104	866.306
19	653	6.4816	20	0.0052	4202.81
20	630	6.4457	23	0.00598	4662.99
22	618	6.4265	12	0.00312	2386.53
24	603	6.4019	15	0.0039	2910.75
28	590	6.3801	13	0.00338	2468.26
32	562	6.3315	28	0.00728	5063.97
36	530	6.2729	32	0.00832	5457.86
40	515	6.2442	15	0.0039	2485.96
44	492	6.1985	23	0.00598	3641.58
48	480	6.1738	12	0.00312	1853.61
52	468	6.1485	12	0.00312	1807.27
60	447	6.1026	21	0.00546	3020.81

This typical polymerization run (Table 4.1) was carried out for 60 minutes at 40°C using $[Cr_3O(F_3CCO_2)_6.3H_2O]NO_3.H_2O$ / $AlEt_2Cl$ catalytic system with 0.0845 g of chromium complex (% Cr = 15.8503 %). Toluene and $AlEt_2Cl$ (0.9 M in toluene) were added successively to the above amount of chromium compound and the total mixture of 400 mL was left to "age" for 40 minutes before being followed by the polymerization of ethylene with stirrer speed of 300 rpm. The corresponding drop in monomer pressure (column four) was recorded every 30 seconds in a computer equipped with Labview software and the catalytic activity was expressed in units of weight of polyethylene formed per weight of Cr used in one hour at atmospheric pressure. Figure 4.1 shows the drop of ethylene pressure versus reaction time and Figure 4.2 shows the plot of ln P versus reaction time.

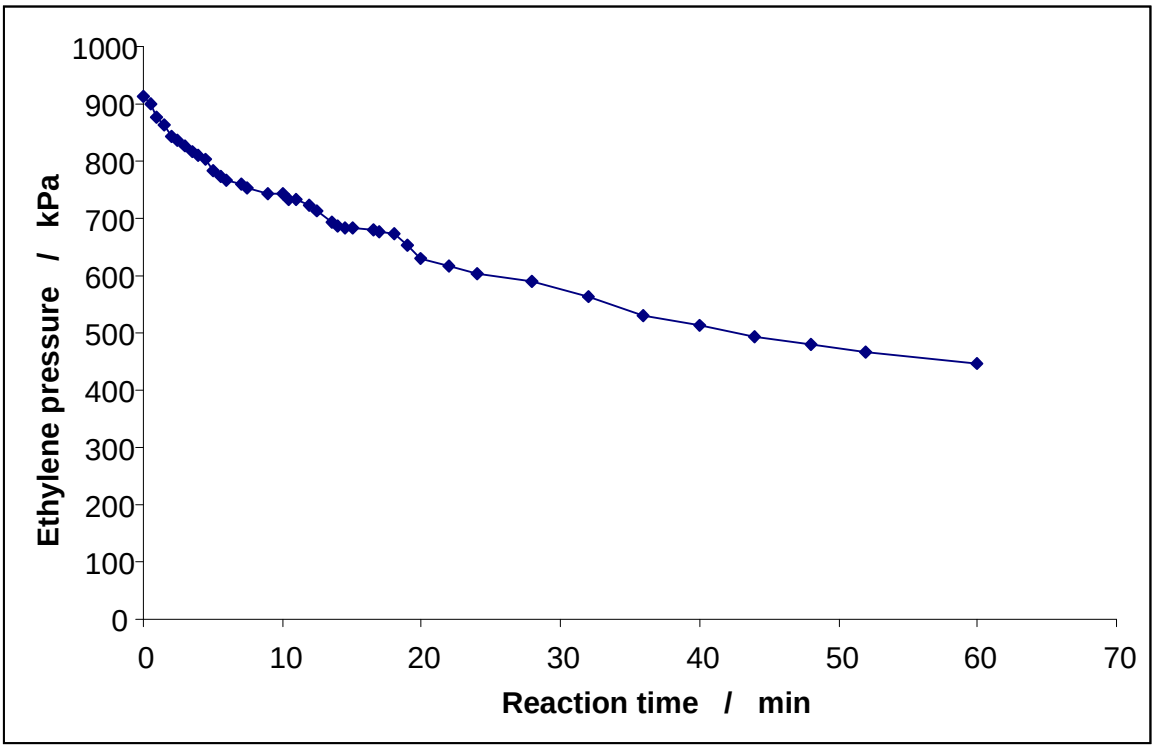

Figure 4.1: A plot of monomer pressure vs. reaction time for the polymerization of ethylene.

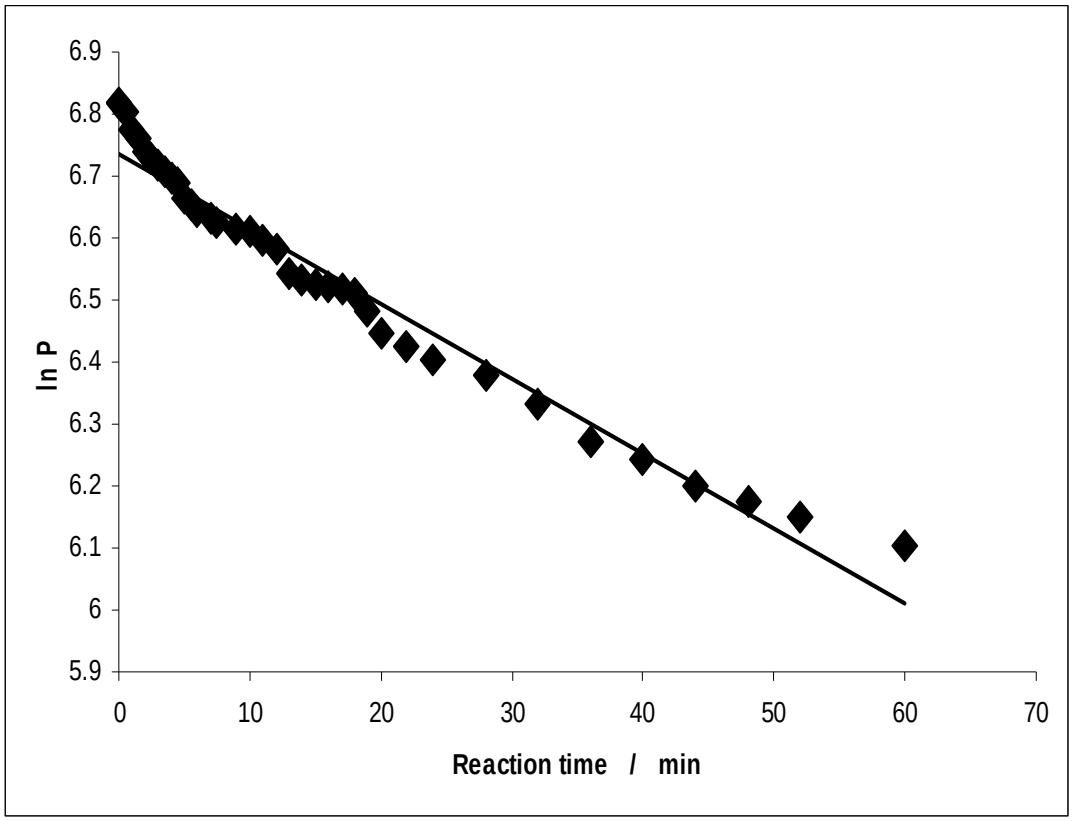

Figure 4.2: A plot of ln P versus reaction time for ethylene polymerization.

The linear graph of ln P versus reaction time confirms the reaction to be of first order and the gradient of the graph is equal to –k, where k is the overall rate constant.

To investigate the effects of monomer pressure and Cr / Al ratio on the polymer yield, reaction rate and catalytic activity respectively, five series of experiments were carried out (Table 4.2) in which the initial monomer pressure was varied from 93-1320 kPa. Each series was carried out with a 1000 mL reactor , at 40 ^{o}C using about 0.08 g of the chromium complex and constant Al/Cr ratio of 20 (series H), 30 (series G), 35 (series I), 45 (series J) and 50 (series K).

Table 4.2: Polymerization data from variable initial monomer pressures and Al/Cr ratios

Cr:Al ratio	P_0 (kPa)	ΔP (kPa)	Experimental yield (g)	Theoretical Yield (g) *	% yield
Series H					
1 :20	440	62	0.42	0.44	95
1 :20	530	82	0.59	0.59	100
1 :20	667	98	0.68	0.70	97
1 :20	865	115	0.83	0.82	~100
1 :20	941	133	0.95	0.95	100
Series G					
1 :30	384	110	0.80	0.83	96
1 :30	500	167	1.23	1.26	98
1 :30	730	180	1.35	1.36	99
1 :30	825	215	1.60	1.63	98
1 :30	855	290	2.25	2.20	~100
1 :30	913	466	3.49	3.53	99
Series I					
1 :35	529	92	0.59	0.66	89
1 :35	689	110	0.75	0.79	95
1 :35	844	121	0.83	0.87	95
1 :35	863	123	0.85	0.88	97
1 :35	947	357	2.20	2.56	86
Series J					
1 :45	342	45	0.33	0.32	~100
1 :45	675	69	0.41	0.49	84
1 :45	822	85	0.60	0.61	98
1 :45	931	134	0.95	0.96	99
1 :45	1320	460	3.21	3.29	98
Series K					
1 :50	93	5	0.04	0.04	100
1 :50	286	7	0.05	0.05	100
1 :50	445	44	0.32	0.34	94
1 :50	869	86	0.62	0.62	100
1 :50	1083	99	0.72	0.72	100

* = theoretical yield calculated from the number of moles (Δn) of ethylene reacted. $\Delta n = \Delta P(V/RT)$.

4.3 Effect of monomer pressure

4.3.1 Correlations between the monomer pressure change and polymer yield.

The correlation between the change in ethylene pressure and the polymer yield was investigated using each series of the polymerization data in Table 4.2. In each group, the polymerization reactions were carried out with different initial monomer pressures and constant Cr / Al ratio. The corresponding drops in ethylene pressure and polymer yield were determined. One example of a plot of experimental yield versus theoretical yield is depicted in Figure 4.3. This graph, which shows a linear correlation between the experimental yields versus theoretical yields, was obtained from the data of "series G" where Cr / Al ratio is 1 / 30. In addition, similar results were observed with all other series.

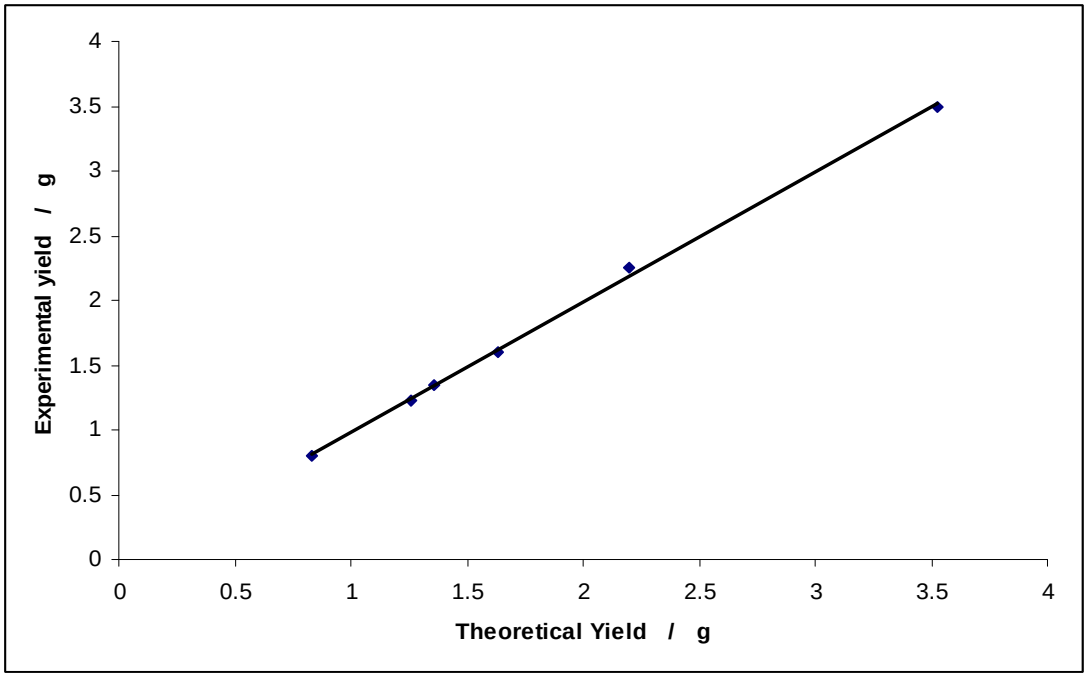

Figure 4.3: Plot of experimental yield versus theoretical yield using $[Cr_3O(F_3CCO_2)_6.3H_2O]NO_3.H_2O$ / $AlEt_2Cl$ catalyst system, Cr/Al ratio = 1/30.

4.3.2 Effect of monomer pressure on polymer yield

The effect of different monomer pressures on the amount of polymer product was studied. Figure 4.4 shows the effect of different initial ethylene pressures on the amount of polyethylene produced. The plot was obtained from the data of "series G" (Table 4.2) equivalent to Cr/Al ratio of 1/30. As can be observed in this plot, the higher the initial monomer pressure, the bigger the amount of high density polyethylene produced. Similar observations are obtained for the four other series.

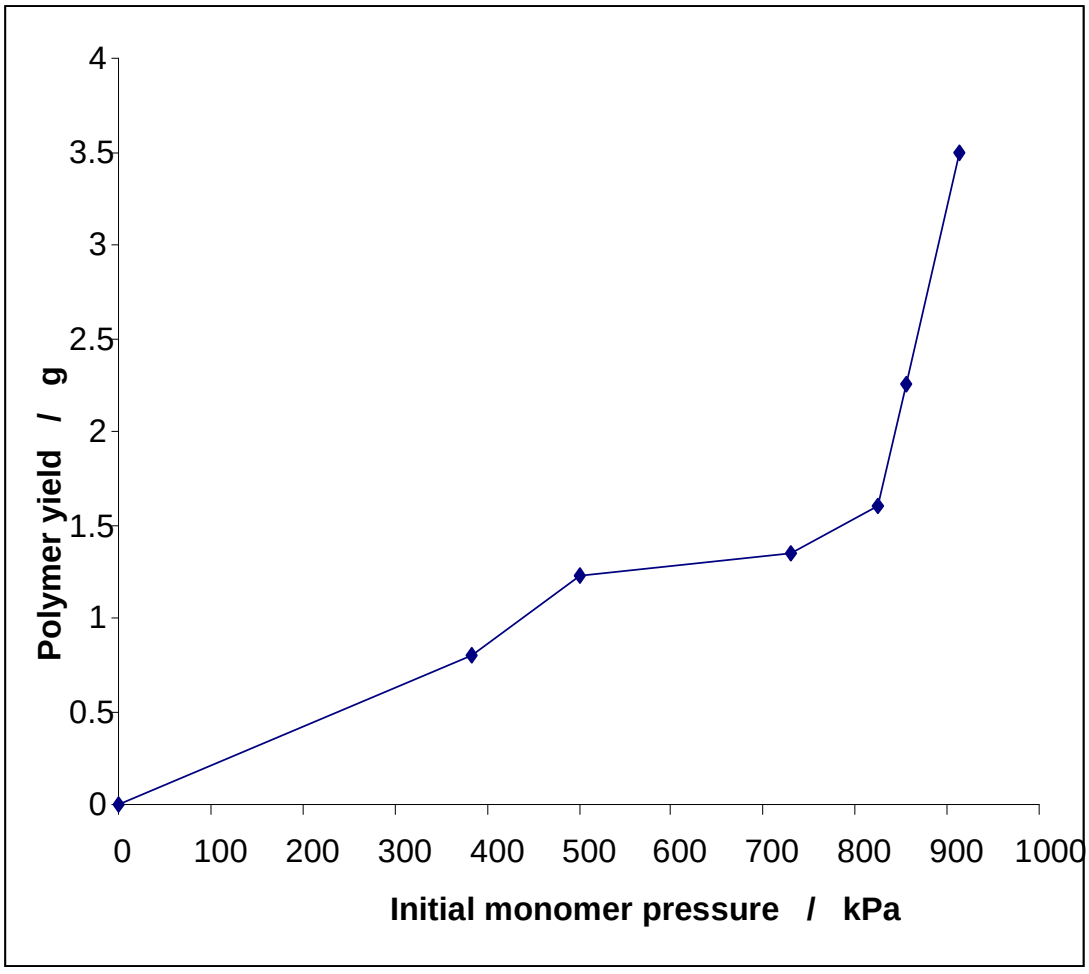

Figure 4.4: Plot of the effect of initial monomer pressure versus polymer yield using $[Cr_3O(F_3CCO_2)_6.3H_2O]NO_3.H_2O$ / $AlEt_2Cl$ catalyst system and Cr/Al ratio of 1/30

Moreover, a plot of accumulated yield, against reaction time, is shown in Figure 4.5. It is observed that the production of PE increases rapidly for the first five minutes, hence the linear correlations seen in the graph. In addition, the initial ethylene pressure influences the amount of polymer produced; the higher the monomer pressure, the bigger the amount of polymer.

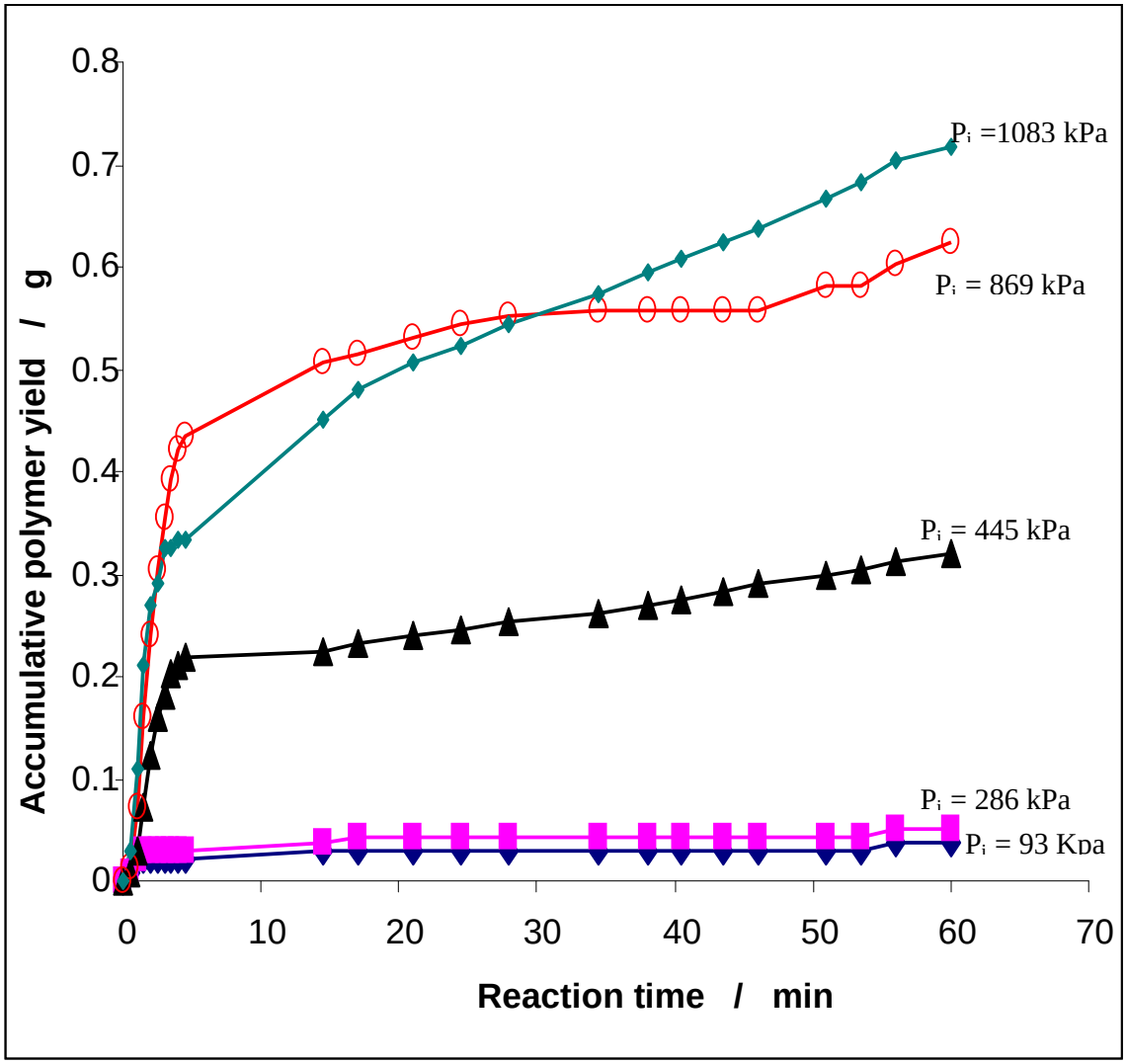

Figure 4.5: Plot of accumulative yield versus reaction time using $[Cr_3O(F_3CCO_2)_6.3H_2O]NO_3.H_2O$ / $AlEt_2Cl$ catalyst system with Cr/Al ratio of 1/50 and initial monomer pressures of 93, 286, 445, 869 and 1083 kPa respectively

4.3.3 Effect of monomer pressure on reaction rate

The studies of the kinetics of ethylene polymerization outline in section 4.2, reveal that ln P = -kt + c, where k represents the overall rate constant of the polymerization, P the pressure of ethylene at time (t) and c is the intercept of the straight line graph obtained when plotting ln P against reaction time.

To investigate the effect of ethylene pressure on the polymerization rate, a series of experiments were carried out with variable monomer pressure (93 – 1083 kPa). The ratio of Cr/Al was kept at 1:50 (series K, Table 4.2), the weight of $[Cr_3O(F_3CCO_2)_6.3H_2O]NO_3.H_2O$ used was about 0.08 g and the temperature was maintained at 40 ^oC.

As expected, the plot of ln P against the reaction time shows that the gradient increases with the higher initial monomer pressure (Figure 4.6). A plot of the intercept "c", from the graph ln P = -kt+c versus the calculated values of ln (P_i) shows a linear correlation (Figure 4.7). This means that the calculated values of logarithm of initial monomer pressures agree well with the intercepts of the graphs. They are summarized in Table 4.3 together with the values of the gradients at variable initial ethylene pressure P_i.

Table 4.3: Effect of monomer pressure on reaction rate

P_i (kPa)	Gradient x (-1) = k	Intercept "c" from the graphs	value of "c" by calculation
93	0.0142	4.5163	4.5326
286	0.0121	5.649	5.6560
445	0.0106	6.0875	6.0981
869	0.0058	6.7583	6.7673
1083	0.0047	6.9745	6.9875

$[Cr_3O(F_3CCO_2)_6.3H_2O]NO_3.H_2O$ / $AlEt_2Cl$ catalyst system, temperature of 40 ^oC, stirrerspeed of 300 rpm and Al /Cr ratio of 50

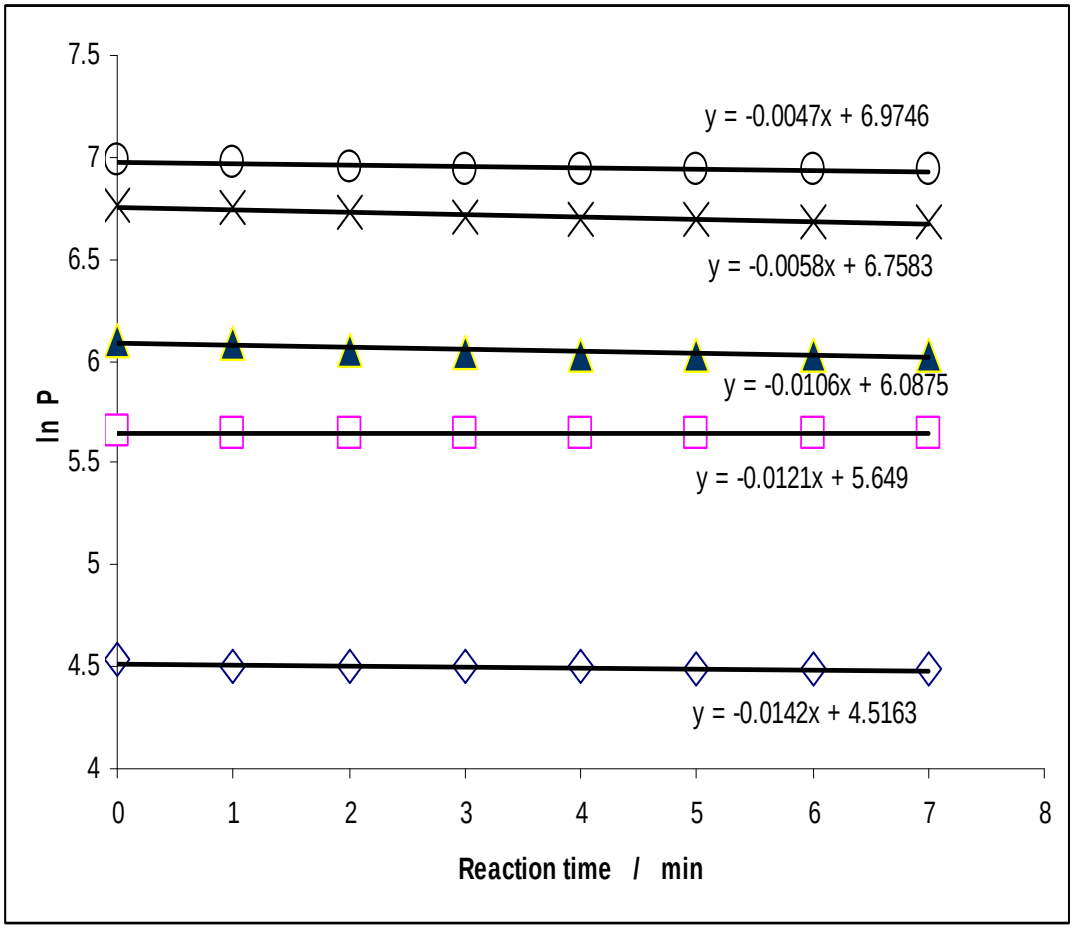

Figure 4.6: Effect of initial monomer pressure on the polymerization of ethylene using $[Cr_3O(F_3CCO_2)_6.3H_2O]NO_3.H_2O$ / $AlEt_2Cl$ catalyst system with temperature of 40^oC, stirrer speed of 300 rpm Cr/Al ratio of 1/50 and initial monomer pressure of 93, 286, 445, 869 and 1083 kPa respectively

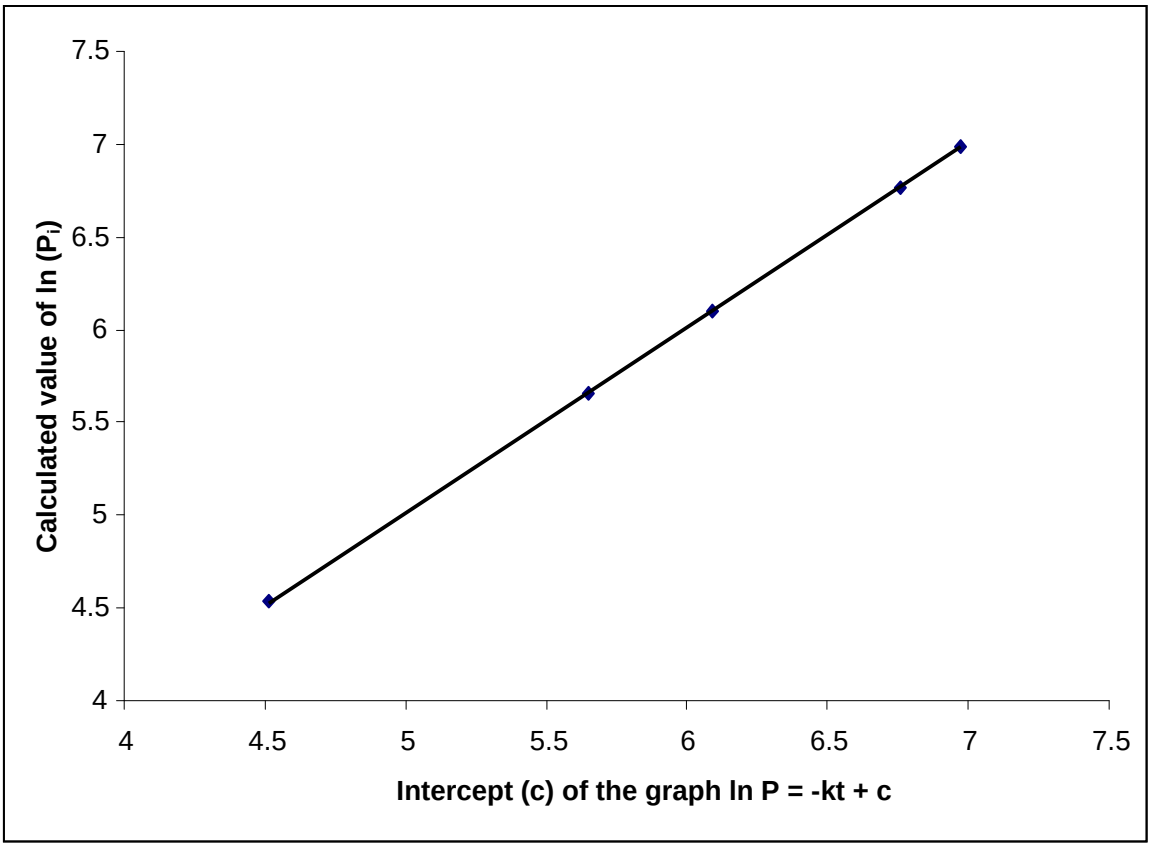

Figure 4.7: Plot of intercept (c) from the graph (ln P = -kt + c) versus the calculated value of ln P_i, where P_i is the initial monomer pressure of the polymerization.

4.3.4 Effect of monomer pressure on catalytic activity

The effect of initial ethylene pressure on the activity of the $[Cr_3O(F_3CCO_2)_6.3H_2O]NO_3.H_2O$ / $AlEt_2Cl$ catalytic system was investigated at constant Al/Cr ratio of 45 (series J, Table 4.2) , temperature of 40 ^oC and variable initial monomer pressures. The maximum initial activity of each experiment was noted (Table 4.4) and a plot of activity against initial ethylene pressure is shown in Figure 4.8.

Table 4.4: Catalyst activity obtained at various initial monomer pressures (P_i)

Run	P_i (kPa)	Maximum initial activity (g-PE/g-Cr/hr/atm)
1	342	1405
2	675	1738
3	822	2643
4	931	5784
5	1320	13859

$[Cr_3O(F_3CCO_2)_6.3H_2O]NO_3.H_2O$ / $AlEt_2Cl$ catalyst system, temperature = 40^oC, stirrer speed =300 rpm, Al /Cr ratio = 45

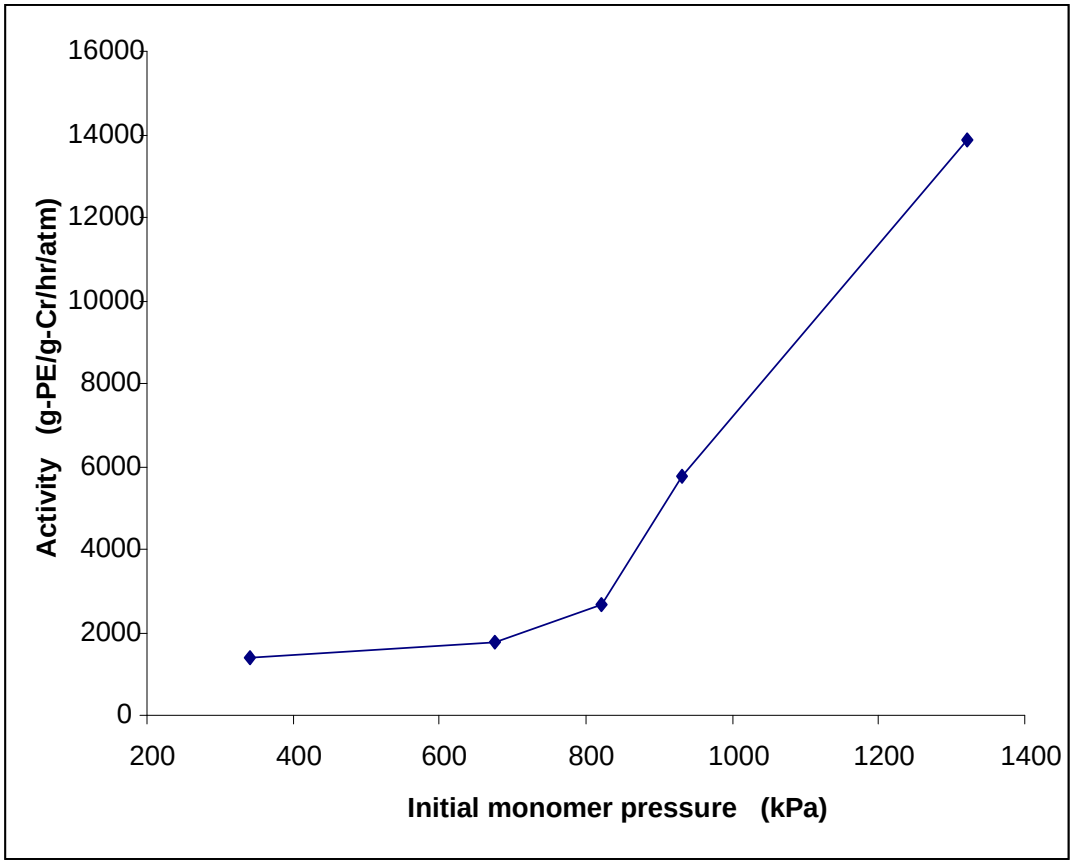

Figure 4.8: Effect of pressure on catalyst activity, temperature of 40 ^oC, Al /Cr ratio of 45 using $[Cr_3O(F_3CCO_2)_6.3H_2O]NO_3.H_2O$ / $AlEt_2Cl$ catalyst system

The above data (Table 4.4) reveals that the catalytic system is highly dependent on the initial monomer pressure. For this series of experiments (series J, Table 4.2), an increase in the ethylene pressure from 342 kPa to 1320 kPa raises the maximum initial activity from 1.4 Kg-PE/g-Cr/hr/atm to 13.9 Kg-PE/g-Cr/hr/atm. This may be due to the fact that as pressure increases it gives higher monomer concentration; the insertion of monomer should be more rapid and thus higher activity of the catalyst. Similar observations have been reported previously [8, 9].

Figure 4.9 shows the catalyst behavior as a function of reaction time using the above catalytic system. These curves are characterized by three different parts:

- The formation of active centers

This step is observed for the first seventeen minutes of the reaction. Here the interaction of the cocatalyst ($AlEt_2Cl$) with the surface of the chromium(III) complex resulted in the reduction of Cr(III) to Cr(II), thus activating the chromium centers [10]. Formation of active centers increases the polymerization rate, hence the very exothermic reaction observed during the polymerization experiments. It is important to point out that the kinetic curves for ethylene polymerization (Figure 4.9) show that we have more than one active site. This is reflected by the presence of more than one peak in the curve for each experiment.

- The steady period

The polymerization rate is observed to decrease after the activation period. This steady state is observed to last for about 38 minutes. In addition, it confirms that the active sites of the catalyst cannot remain active forever as reported by Burnett et al. [4].

- Catalyst deactivation

This step is observed in the last five minutes of the reaction. This deactivation step may be due to the individual destruction of active centers or due to the accumulation of catalyst particles onto the polymer in the solution [11, 12].

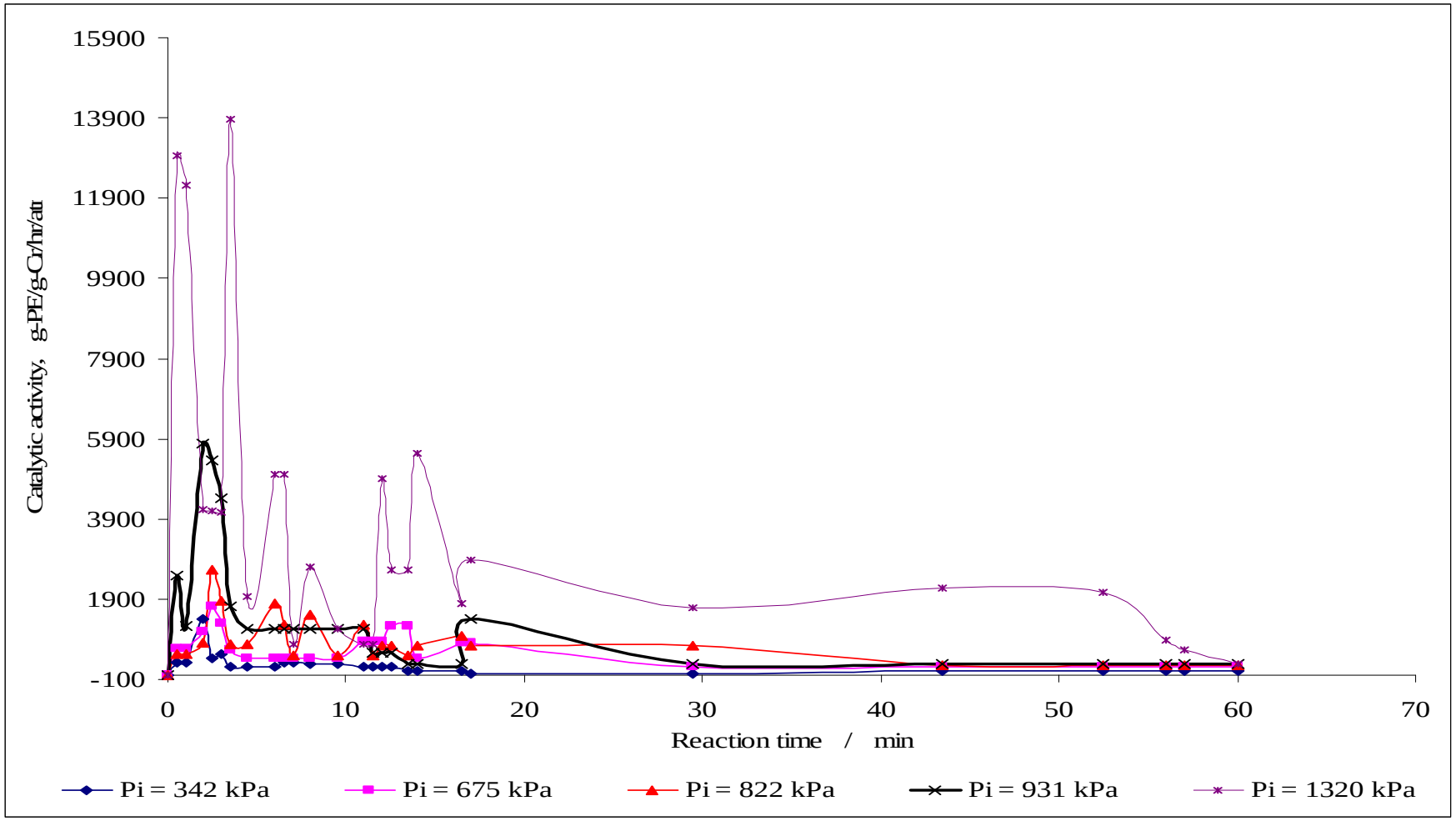

Figure 4.9: Kinetic curves of ethylene polymerization at 40°C, Al /Cr ratio = 45, stirrer speed of 300 rpm and variable initial ethylene pressures using $[Cr_3O(F_3CCO_2)_6.3H_2O]NO_3.H_2O$ / $AlEt_2Cl$ catalyst system

4.4 Effect of varying aluminum / chromium ratio

The influence of the cocatalyst to chromium complex ratio (Al / Cr ratio) was investigated using a series of experiments in which the initial monomer pressure was similar but the concentrations of $AlEt_2Cl$ were varied (Table 4.5). About 0.08 g of chromium complex was used at 40 ^oC with a stirrer speed of 300 rpm.

Table 4.5: Catalyst activity obtained at various Al / Cr ratios

Run	Al / Cr ratio	P_i (kPa)	Maximum initial activity (Kg-PE/g-Cr/hr/atm)
1	20	865	3.645
2	30	855	6.883
3	35	863	5.155
4	45	869	3.682
5	50	869	3.400

$[Cr_3O(F_3CCO_2)_6.3H_2O]NO_3.H_2O$ / $AlEt_2Cl$ catalyst system, temperature of 40^oC, stirrer speed of 300 rpm

The activity of the catalyst was found to be highly dependent upon of the Al / Cr ratio (Figures 4.10 and 4.11). The activity of the catalysts increases from the value of Al / Cr equals to 20 up to a maximum at Al / Cr equals to 30 (Figure 4.10). It then decreases as the amount of $AlEt_2Cl$ increases (Table 4.5). The kinetic profile of the catalyst as a function of reaction time shows that activity spikes at the start of the reaction, then has a steady state for about 20 minutes before dropping off (Figure 4.11). These kinetics are similar to a decay type previously reported [13-15]. The decrease in catalyst activity may be interpreted as the excess of $AlEt_2Cl$ over-reducing the active Cr^{2+} to inactive Cr^+ or Cr^0 as reported by Schnecko et al.[16].

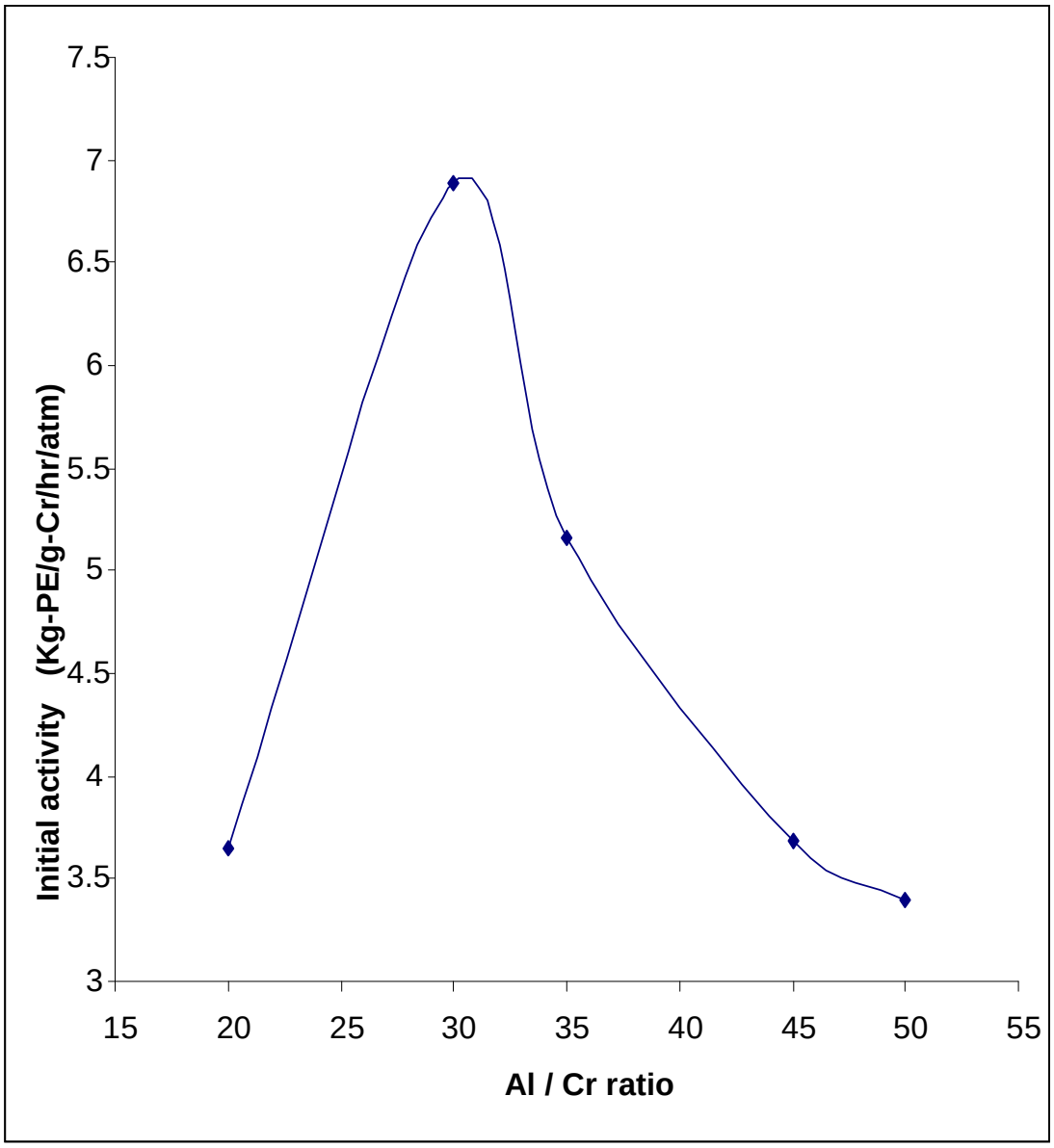

Figure 4.10: Initial catalytic activity as a function of Al / Cr ratio for the polymerization of ethylene at 40 ^{o}C, stirrer speed of 300 rpm and constant initial ethylene pressure using $[Cr_3O(F_3CCO_2)_6.3H_2O]NO_3.H_2O$ / $AlEt_2Cl$ catalytic system

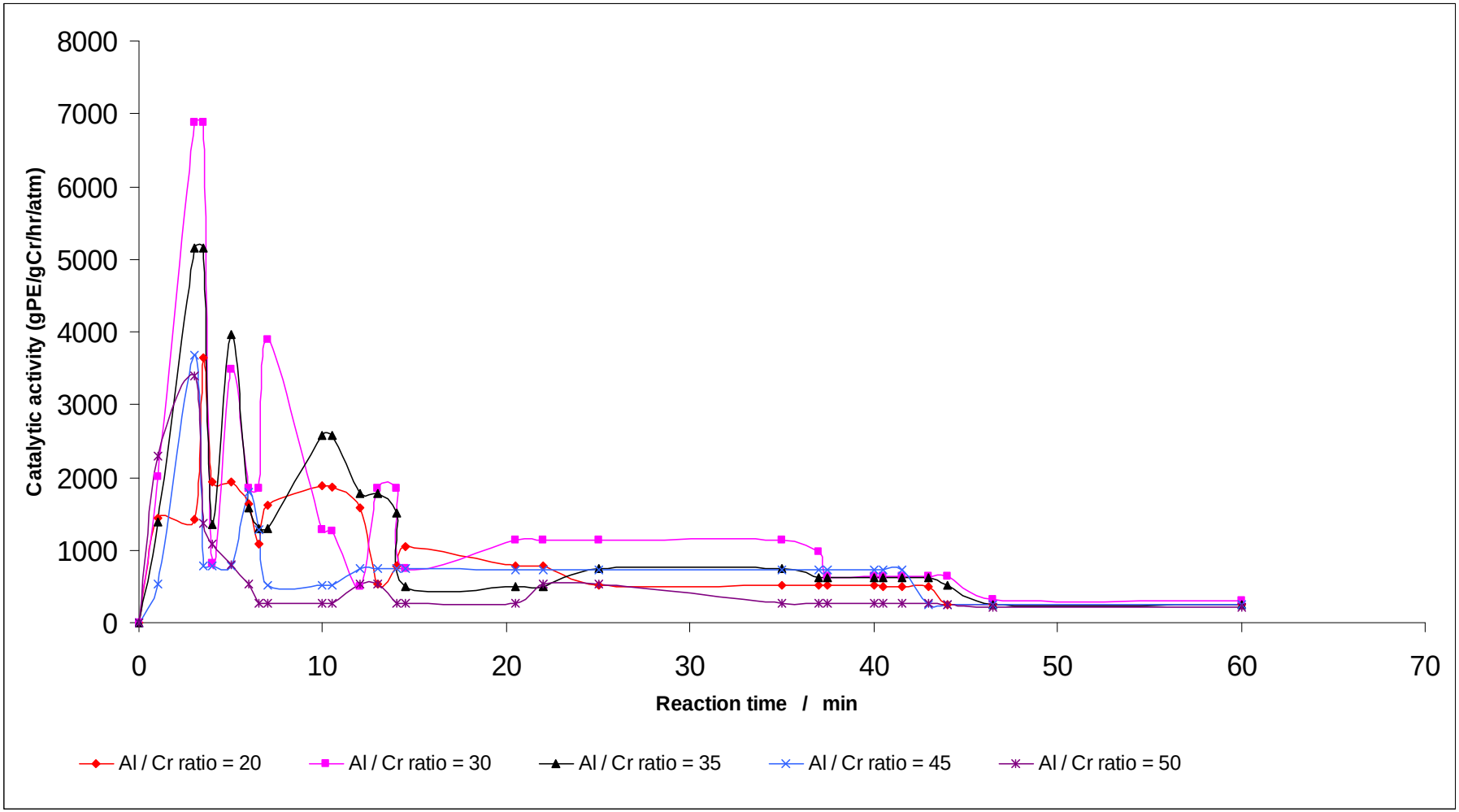

Figure 4.11: Kinetic curves of ethylene polymerization at 40 ^{o}C, stirrer speed of 300 rpm, constant initial ethylene pressure and variable Al /Cr ratios using $[Cr_3O(F_3CCO_2)_6.3H_2O]NO_3.H_2O$ / $AlEt_2Cl$ catalytic system

4.5 Characterization of polymers

The preparations of polymers were closely followed by their characterizations. The results presented here help, not only identify the type of polyethylene produced, but also to facilitate further study of the catalyst activity.

4.5.1 Morphology

An optical microscope and Phenom desktop scanning electron microscope (PHENOM SEM) were used to visualize the polymer morphology. The polymer was white in color, flat and homogenous in shape when looked with an optical microscope (Figure 4.12-a). In addition, the PHENOM SEM micrograph (Figure 4.12-b) shows well defined lamellae [47]. In addition, there is no trace of catalyst particles in the polymer. This means that the $[Cr_3O(F_3CCO_2)_6.3H_2O]NO_3.H_2O$ / $AlEt_2Cl$ catalytic system is highly active and does not required any catalyst removal from the product. The polymer produced is of good purity.

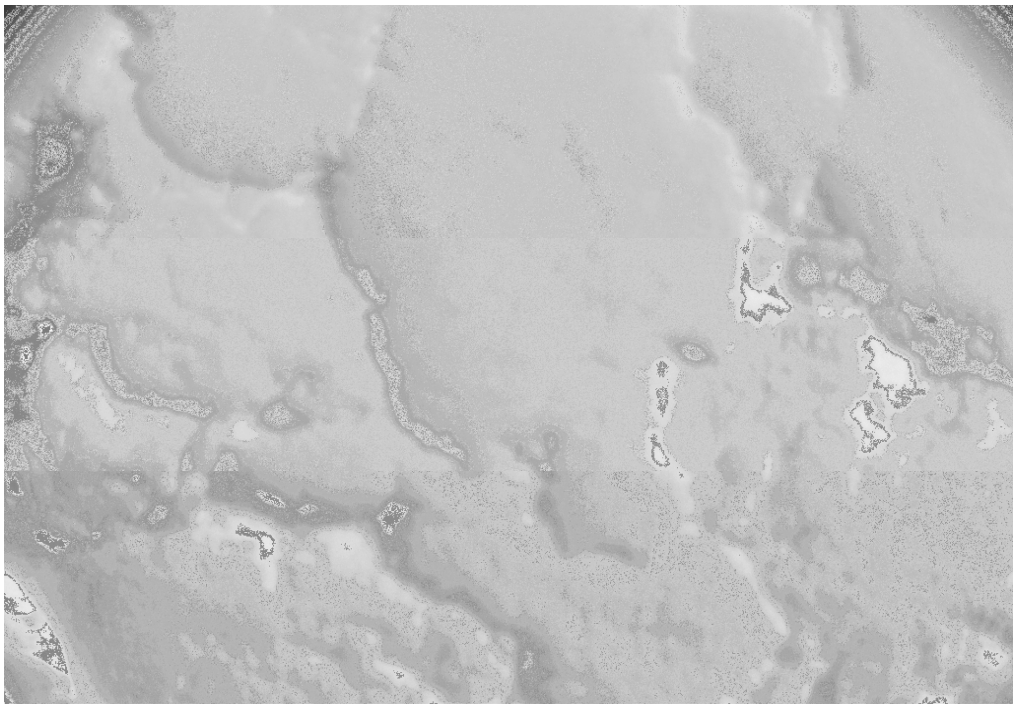

(a)

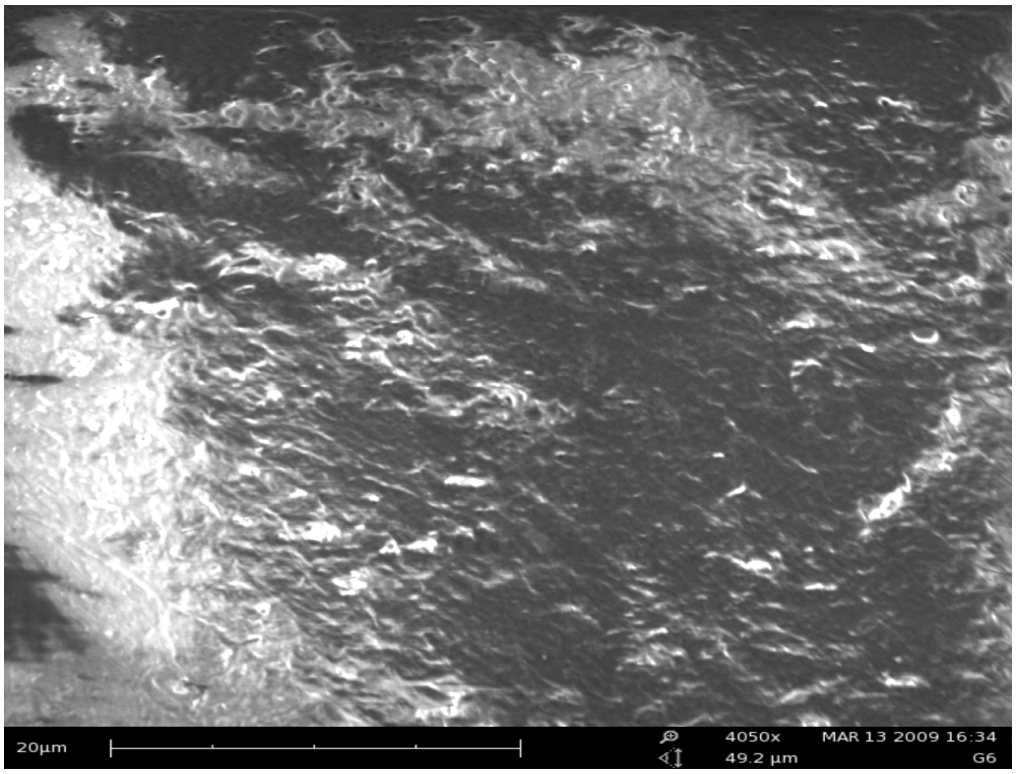

(b)

Figure 4.12: (a) Optical micrograph, (b) PHENOM SEM imaging at magnification of 4050 of the polyethylene from $[Cr_3O(F_3CCO_2)_6.3H_2O]NO_3.H_2O$ / $AlEt_2Cl$ catalytic system

4.5.2 Fourier Transform Infrared spectroscopy (FTIR)

Nowadays, FTIR is probably the most extensively used characterization method for studying polymer structure. This is because it helps in determining functional groups present, in crystallinity measurements and in branching studies of polymers.

Polyethylene has the simplest polymer structure which is a chain of methylene units terminated on each end by methyl groups. Since this polymer consists almost completely of methylene groups, its infrared spectrum is expected to be composed solely of methylene stretches and bends. The methylene stretched bands appear at 2920 cm^{-1} and 2850 cm^{-1} and its deformation modes at 1464 cm^{-1} and 719 cm^{-1}. However, due to the crystallinity of polyethylene, the 1464 cm^{-1} and 719 cm^{-1} peaks are split, and additional peaks are seen at 1473 cm^{-1} and 731 cm^{-1} [17].

Here, the spectra were recorded in the range of 4000 cm^{-1} to 650 cm^{-1}. The samples (5 – 20 mg) were pressed onto a Perkin Elmer spectrum 400 FT-IR / FT-NIR spectrometer. The spectra show six important bands around 2916 cm^{-1}, 2849 cm^{-1}, 1473 cm^{-1}, 1463 cm^{-1}, 730 cm^{-1} and 719 cm^{-1}. A representative spectrum of a sample of polyethylene is shown in Figure 4.13. The sample was produced at 40 ^{o}C using the $[Cr_3O(F_3CCO_2)_6.3H_2O]NO_3.H_2O$ / $AlEt_2Cl$ catalytic system.

The two bands around 2916 cm^{-1} and 2849 cm^{-1} were assigned to CH_2 asymmetric and symmetric stretching modes respectively [18]. It is known that the intensities of the IR bands increase linearly with the increase of the carbon chain length [19, 20].

The absorption bands at 1473 cm^{-1} and 1463 cm^{-1} were assigned respectively to CH_2 deformation and symmetric terminal CH_3 deformation.

The two bands at around 730 cm^{-1} and 719 cm^{-1} have been attributed to rocking modes of the CH_2 group as reported by Sheppard and Sutherland [21]. According to them, the double bands at 730 cm^{-1} and 721 cm^{-1}, in the crystalline PE material, arise from inter and intramolecular interactions between nearer molecules in the crystalline phase. It is well known [20, 22] that the crystallinity content in a polyethylene sample can be determined from the intensity ratio of the absorption band at 730 cm^{-1} which is a equivalent to crystallinity absorption band, and the 720 cm^{-1} peak which is sensitive to the amorphous section of the polyethylene sample.

A series of experiments in which the Al / Cr ratio was kept constant and initial ethylene pressure varied, were carried out to investigate the influences of the initial monomer pressure on the crystallinity of polyethylene. Table 4.6 shows the polyethylene absorption frequencies at various pressures and Table 4.7 summarizes the absorption frequencies at 730 cm^{-1} and 720 cm^{-1} for the FTIR spectra of the polyethylene obtained at 40^{o}C, stirrer speed of 300 rpm and 60 minutes of reaction time using the $[Cr_3O(F_3CCO_2)_6.3H_2O]NO_3.H_2O$ / $AlEt_2Cl$ catalytic system. All the polyethylenes obtained are crystalline, exhibiting all the six characteristics bands. In addition, they also have high ratio values of the absorbances at 730 cm^{-1} and 720 cm^{-1}.

Table 4.6: Bands assignments for FTIR spectra of polyethylene at various initial monomer pressures using $[Cr_3O(F_3CCO_2)_6.3H_2O]NO_3.H_2O$ / $AlEt_2Cl$ catalytic system.

Assigned PE vibration mode		Initial monomer pressure (KPa)					
		384	500	730	825	855	913
CH_2 - Stretching	Asymmetric	2916 s	2916 s	2917 s	2916 s	2916 s	2916 s
	Symmetric	2849 s	2849 s	2849 s	2849 s	2849 s	2849 s
CH_2 - deformation		1472 m	1473 m	1473 m	1473 m	1473 m	1473 m
CH_3 – symmetric deformation		1464 m	1464 m	1463 m	1463 m	1463 m	1463 m
CH_2 - rocking		730 m	730 m	730 m	730 m	730 m	730 m
		718 m	719 m	719 m	719 m	719 m	719 m

s = strong, m= medium

Table 4.7: Absorbance ratio of polyethylene at various initial monomer pressures

Al / Cr ratio	Max P_i (kPa)	Intensity (cm^{-1})		A_{730} / A_{719}
		A_{730}	A_{719}	
30	384	0.06	0.11	0.55
30	500	0.04	0.09	0.44
30	730	0.09	0.20	0.45
30	825	0.06	0.09	0.67
30	855	0.03	0.04	0.75
30	913	0.11	0.16	0.69

Where Max P_i is the maximum initial monomer pressure, A_{730} and A_{720} are the absorption at 730 cm^{-1} and 720 cm^{-1} respectively.

Moreover, the study of the crystallinity of the polyethylene, produced at various Al / Cr ratios was carried at constant initial ethylene pressure, stirrer speed of 300 rpm, reaction time of 60 minutes, reaction temperature of 40^oC using the $[Cr_3O(F_3CCO_2)_6.3H_2O]NO_3.H_2O$ / $AlEt_2Cl$ catalytic system, (Table 4.8). One can notice that, as is the case for the initial monomer pressure, all polyethylene produced are of high crystallinity.

Table 4.8: Absorbance ratio of polyethylene at various Al / Cr ratio

Al / Cr ratio	Max P_i (kPa)	Intensity (cm^{-1})		A_{730} / A_{719}
		A_{730}	A_{719}	
20	865	0.06	0.12	0.50
30	855	0.03	0.04	0.75
35	863	0.08	0.15	0.53
45	822	0.07	0.10	0.70
50	869	0.08	0.14	0.57

Where Max P_i is the maximum initial monomer pressure, A_{730} and A_{720} are the absorption at 730 cm^{-1} and 720 cm^{-1} respectively

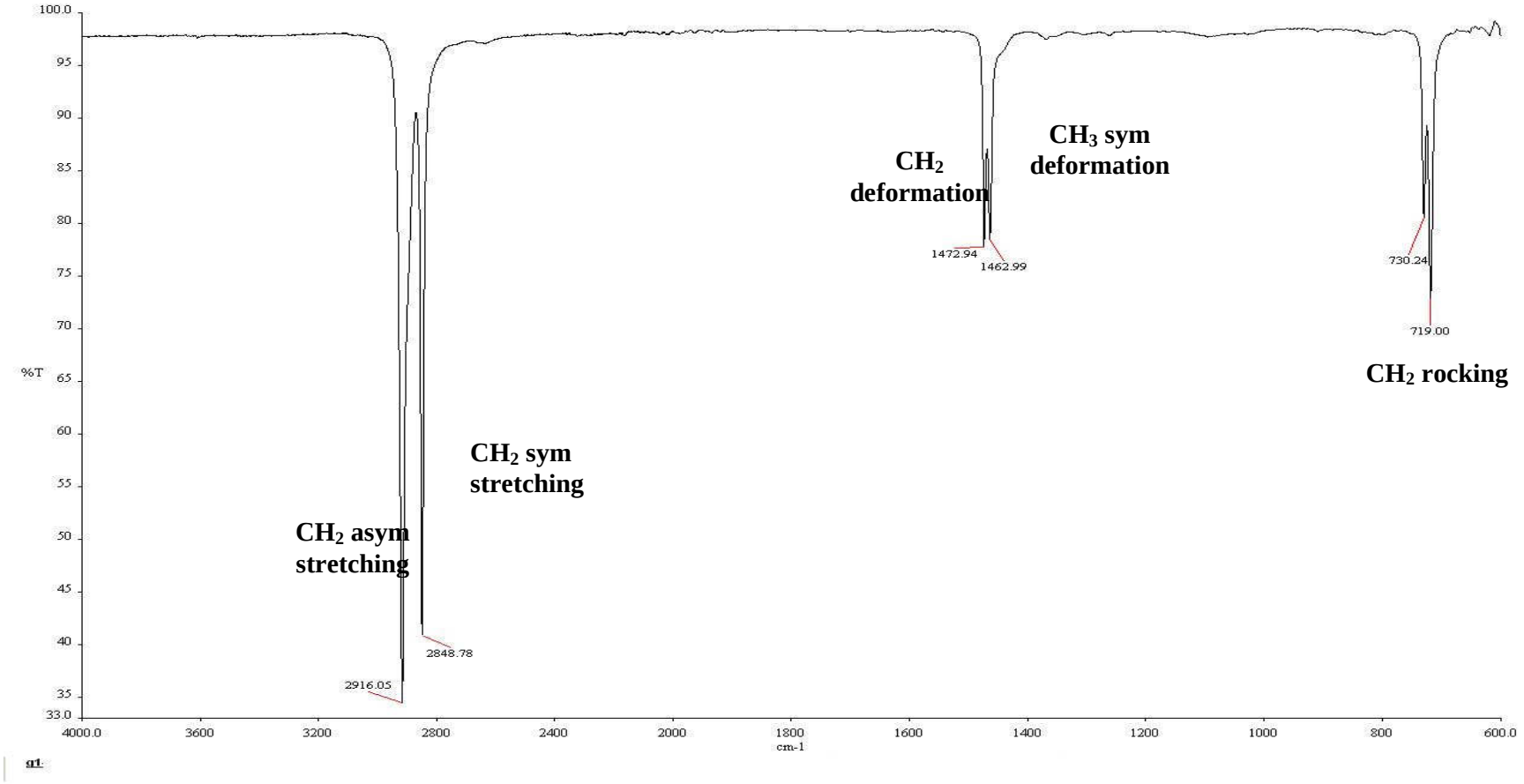

Figure 4.13: FTIR spectrum of PE obtained from $[Cr_3O(F_3CCO_2)_6.3H_2O]NO_3.H_2O$ / $AlEt_2Cl$ catalytic system at Al / Cr ratio of 30 , temperature of 40 ^oC and initial monomer pressure of 825 kPa. Reaction time = 60 minutes

4.5.3 Thermal Gravimetric analysis (TGA)

Thermogravimetric analysis (TGA) measures the mass change in a sample as a function of temperature or time. It is an important technique which provides valuable information on the thermal stability of polymer samples. Here, the thermograms were obtained under nitrogen atmosphere by heating 10 to 20 mg of the polyethylene sample in a temperature range of 50 to 900 ^{o}C.

As seen in Figure 4.14, the polyethylene samples are stable up to the range of 300 – 350 ^{o}C. Above this temperature, they decompose almost completely (95 - 100 %) without any break. This observation can be interpreted as the polyethylenes being of high purity or the chain lengths of their sequence units are reasonably regular. Furthermore, no significant change is observed when the initial monomer pressure is increased or the Al / Cr ratio is varied.

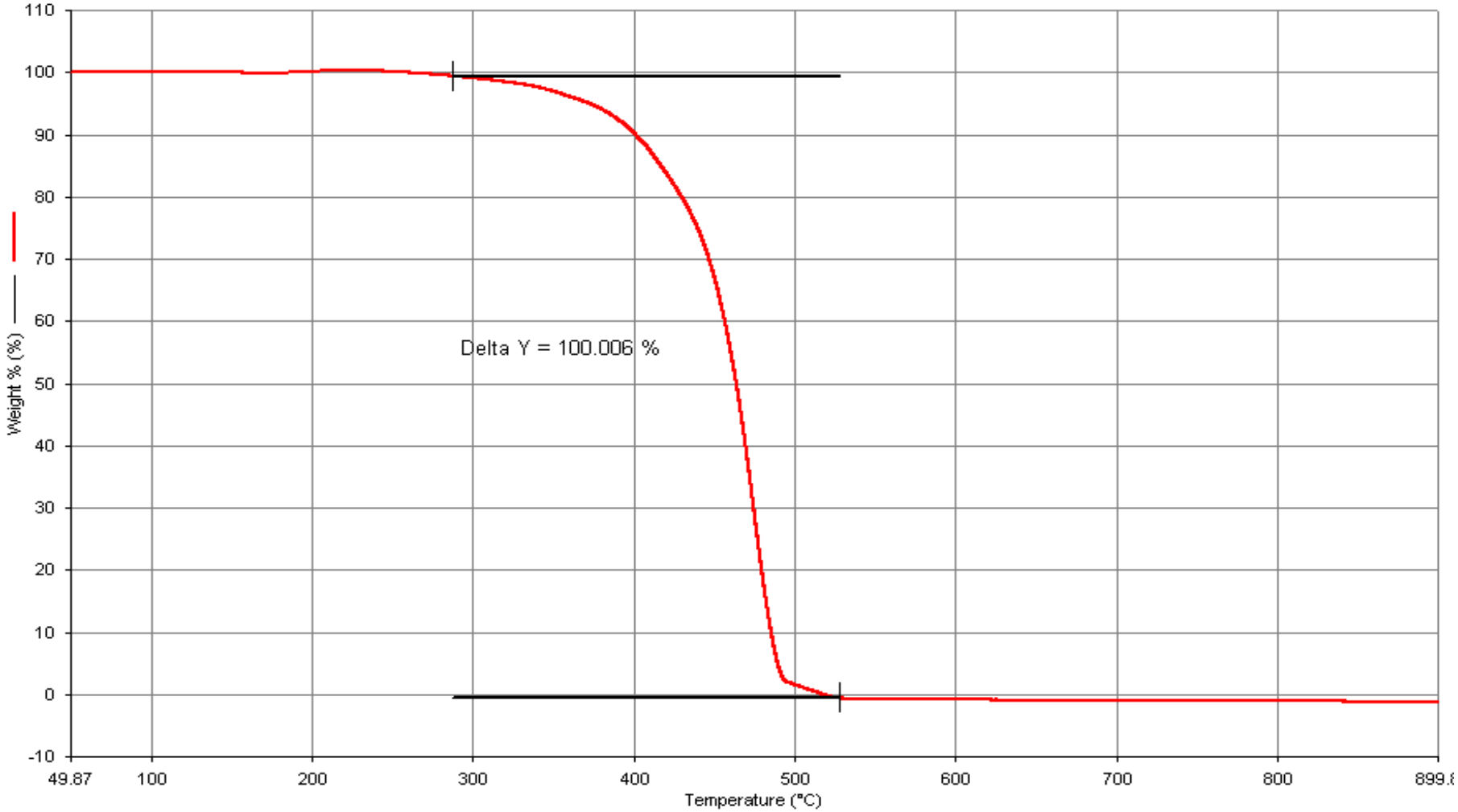

Figure 4.14: A representative TGA thermogram of the decomposition of high density polyethylene in nitrogen; Al / Cr ratio = 30; P= 730 kPa; T = 40 ^{o}C; reaction time = 60 min using $[Cr_3O(F_3CCO_2)_6.3H_2O]NO_3.H_2O$ / $AlEt_2Cl$ catalytic system.

4.5.4 Differential Scanning Calorimetry (DSC)

Melting endotherms were determined using a Perkin-Elmer DSC 6 differential scanning calorimeter (DSC). Indium was used for the calibration of the temperature scale. 5 – 10 mg of purified polyethylene sample were weighed and encapsulated in standard aluminum sample pans. The measurements were carried out at the scanning rate of 10^{o}C/min.Two scans were performed. The first scan was to erase the thermal history of the sample using the DSC cycle of melting followed by cooling with air. The temperatures were recorded from the second scan. The melting temperature as well as the crystallinity (X_c) of the polyethylene matrices are summarized in Table 4.9. The degree of crystallinity was estimated by comparing the measured melting enthalpy (from the second scan) to that of a pure polyethylene crystal (289 J/g) [23, 24].

DSC analyses of PE samples from five series of experiments have been carried out to study the effects of initial monomer pressure and Al / Cr ratio on the melting and crystallization temperatures of the polymers. Their data, summarized in the Table 4.9, reveal that most of the melting peaks from the first scan are broad with melting temperatures in the range of (129 - 147) ^{o}C. After annealing, cooling and reheating, the peaks are sharper but the new melting temperatures are, surprisingly, in the range of (130 - 139) ^{o}C. This drop in melting temperatures may be due to the unordered ethylene unit being aligned in the domains to form crystalline units [25]. This observation is obtained for all the polymer samples except the PE sample from series H where the initial monomer pressure was 440 kPa and the Al / Cr molar ratio of 20. In comparison with others, its melting temperature increases from 129 to 130 ^{o}C, but it was found to have the lowest percentage crystallinity of all polymer samples.

For each series of experiments carried out at constant Al / Cr ratio but different initial monomer pressure, an increase in the initial ethylene pressure affects the

molecular structure of the polyethylene, as shown in Figures 4.15, 4.16 and 4.17, by the increase in the intensity of the DSC curves and in the melting temperature value. Similar observations have been reported by Escher et al. [9] while doing similar studies.

Table 4.10 shows data from a series of experiments, obtained using the above catalytic system with similar initial monomer pressure but variable Al / Cr ratios. As can be seen, the increase in Al / Cr ratio increases the melting temperature of the PE. However, it has little effect on the crystallization temperature ($T_c \approx 113 \pm 1\ ^oC$) except for the sample obtained at Al / Cr ratio 30 which has its $T_c = 116\ ^oC$ with the highest percentage of crystallinity of all samples (80 %). A representative of their first scan, cooling and second scan DSC curves are respectively shown in Figures 4.18, 4.19 and 4.20.

Generally, the polyethylene samples have high melting temperatures, high heat of fusion and therefore high crystallinity. All broad peaks, or peaks with shoulders, obtained in the first scan become sharp after annealing and rescanning. The enthalpy of fusion decreases, after annealing at room temperature from the first to the second DSC scan. This is because the short periods used for annealing the PE samples allow only the crystallization of the shortest ethylene sequences. Consequently, only the more stable lamellae are rearranged and ordered to a better crystalline material. An increase in both initial monomer pressure and Al / Cr ratio increase the melting temperature but have little influence on the crystallization temperature.

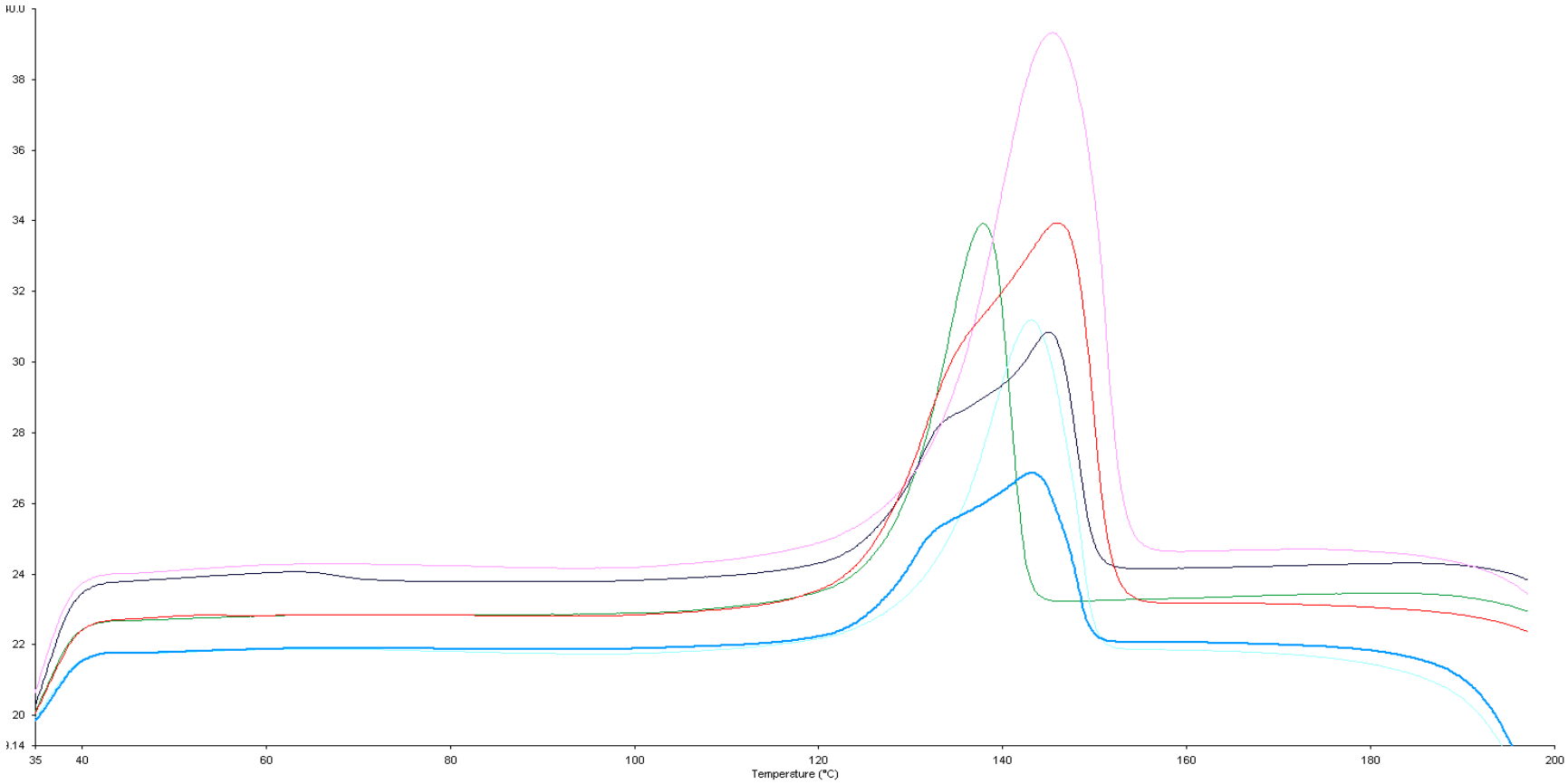

Figure 4.15: Effect of the initial monomer pressure on the first DSC scan of polyethylene samples produced at Al / Cr ratio = 30; P_i = 500, 730, 384, 825, 913 and 855 kPa respectively from bottom to the top; T = 40 ^{o}C; reaction time = 60 min using $[Cr_3O(F_3CCO_2)_6.3H_2O]NO_3.H_2O$ / $AlEt_2Cl$ catalytic system

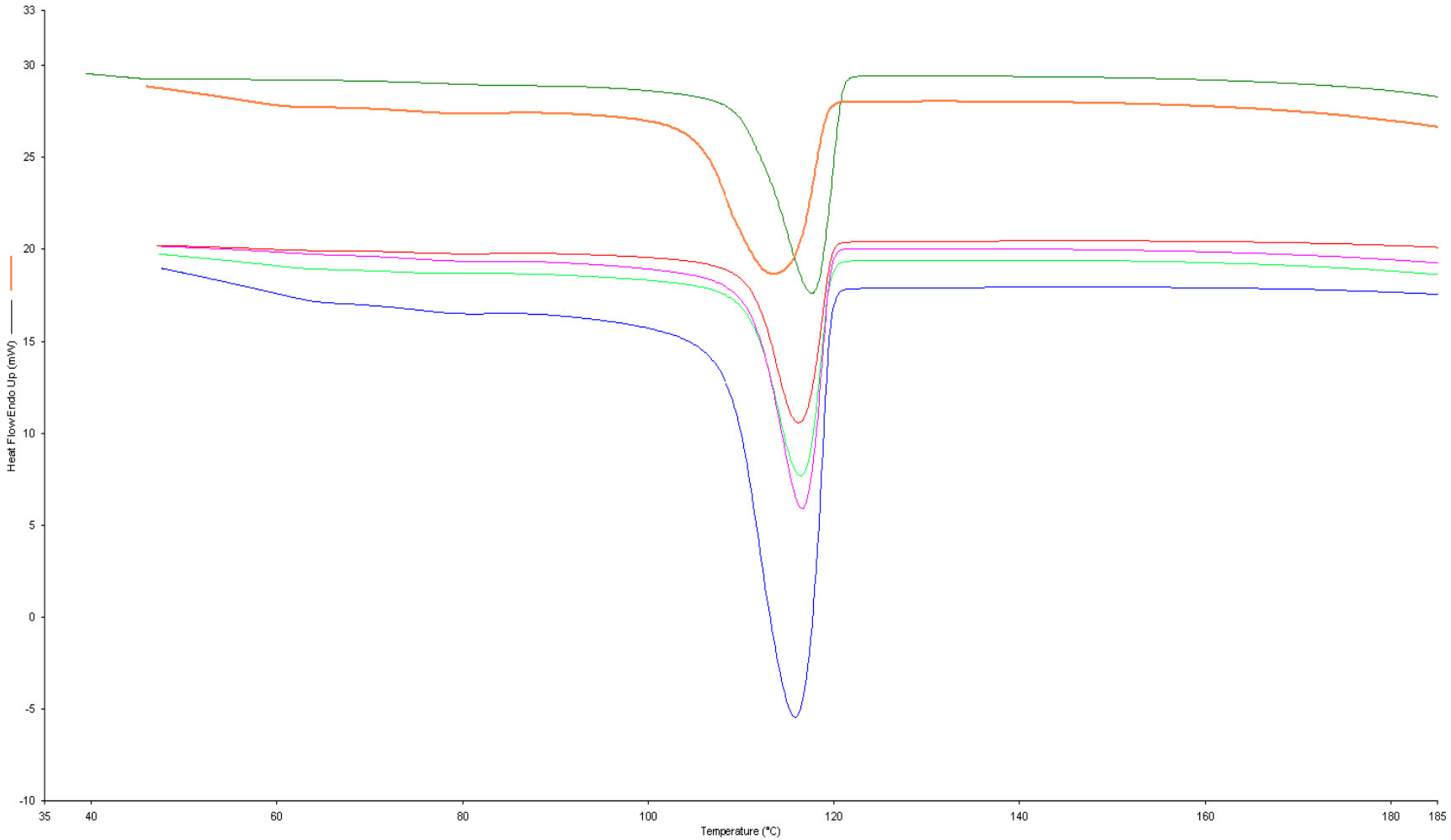

Figure 4.16: Effect of the initial monomer pressure on the cooling DSC scan of polyethylene samples produced at Al / Cr ratio = 30; P_i = 500, 730, 384, 825, 913 and 855 kPa respectively from the top to the bottom; T = 40 ^{o}C; reaction time = 60 min using $[Cr_3O(F_3CCO_2)_6.3H_2O]NO_3.H_2O$ / $AlEt_2Cl$ catalytic system

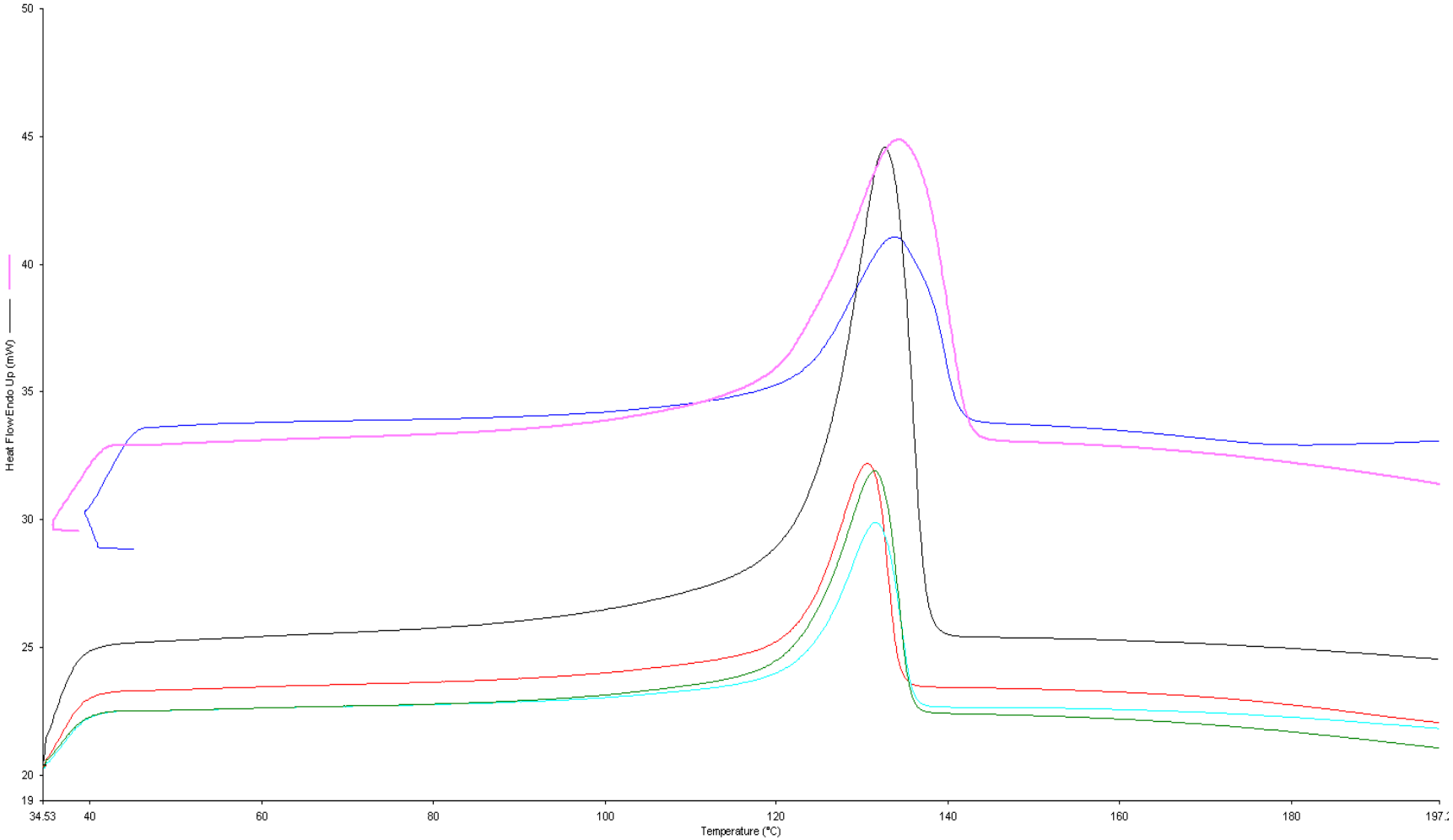

Figure 4.17: Effect of the initial monomer pressure on the second DSC scan of polyethylene samples produced at Al / Cr ratio = 30; P_i = 500, 730, 384, 825, 913 and 855 kPa respectively from bottom to the top; T = 40 ^{o}C; reaction time = 60 min using $[Cr_3O(F_3CCO_2)_6.3H_2O]NO_3.H_2O$ / $AlEt_2Cl$ catalytic system

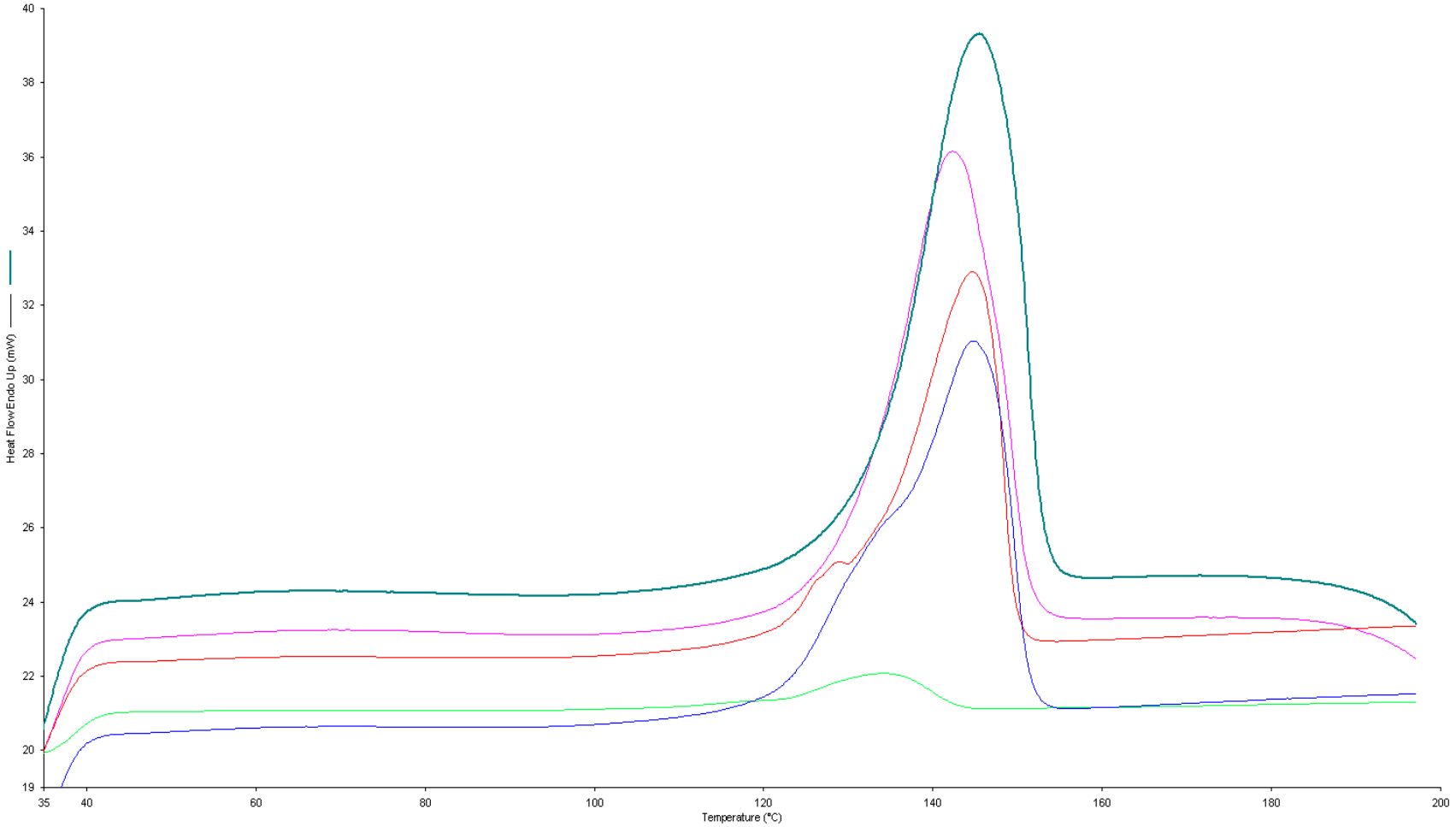

Figure 4.18: Effect of various Al / Cr ratios on the first DSC scan of polyethylene samples produced at Al / Cr ratio = 20, 35, 50, 45 and 30 respectively; $P_i \approx 855$ kPa from bottom to the top using $[Cr_3O(F_3CCO_2)_6.3H_2O]NO_3.H_2O$ / $AlEt_2Cl$ catalytic system reaction, at T = 40 °C and 60 min reaction time

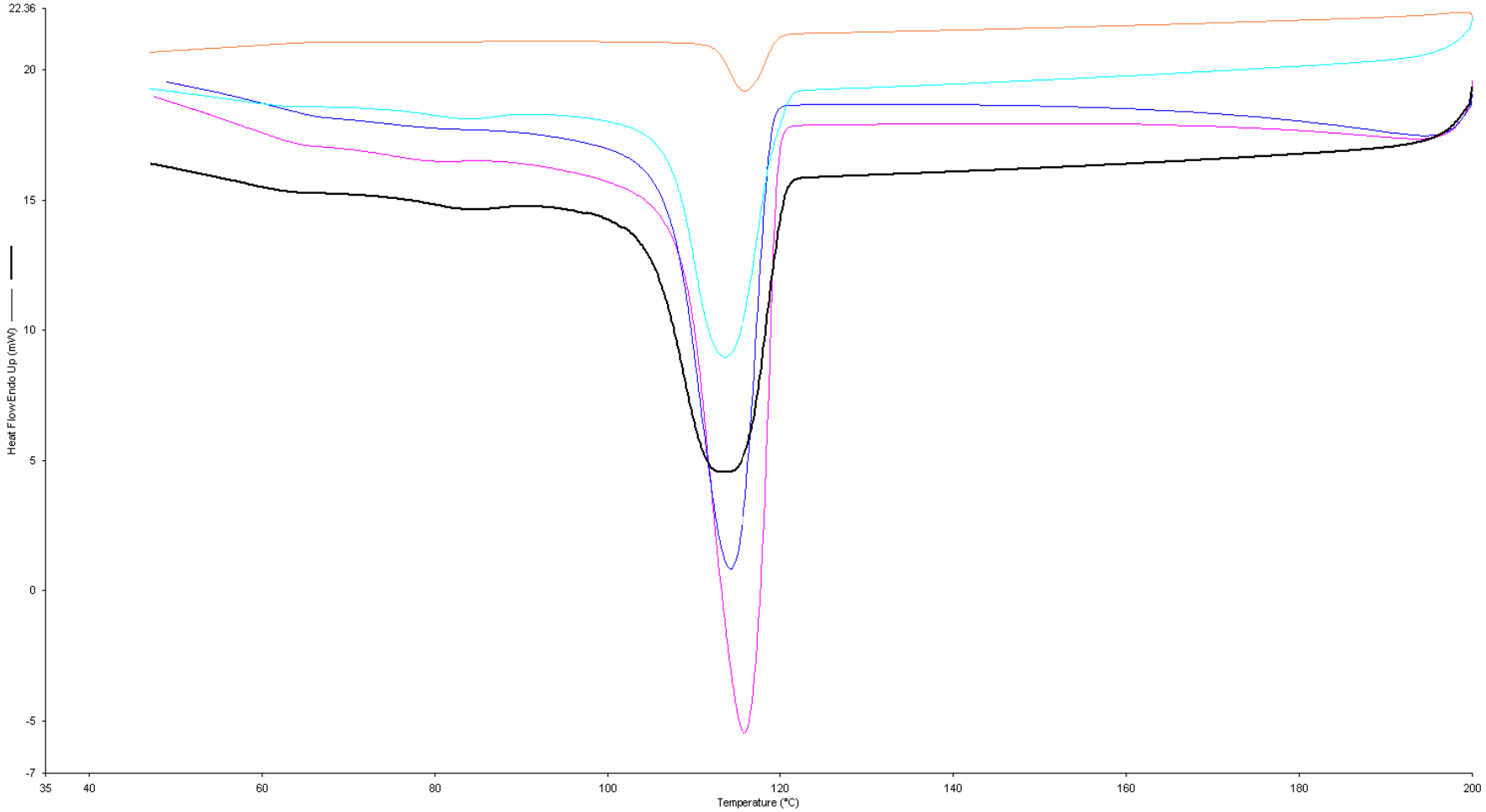

Figure 4.19: Effect of various Al / Cr ratios on the cooling DSC scan of polyethylene samples produced at Al / Cr ratio = 20, 35, 50, 45 and 30 respectively; $P_i \approx 855$ kPa from the top to the bottom using $[Cr_3O(F_3CCO_2)_6.3H_2O]NO_3.H_2O$ / $AlEt_2Cl$ catalytic system reaction, at T = 40 ^oC and 60 min reaction time

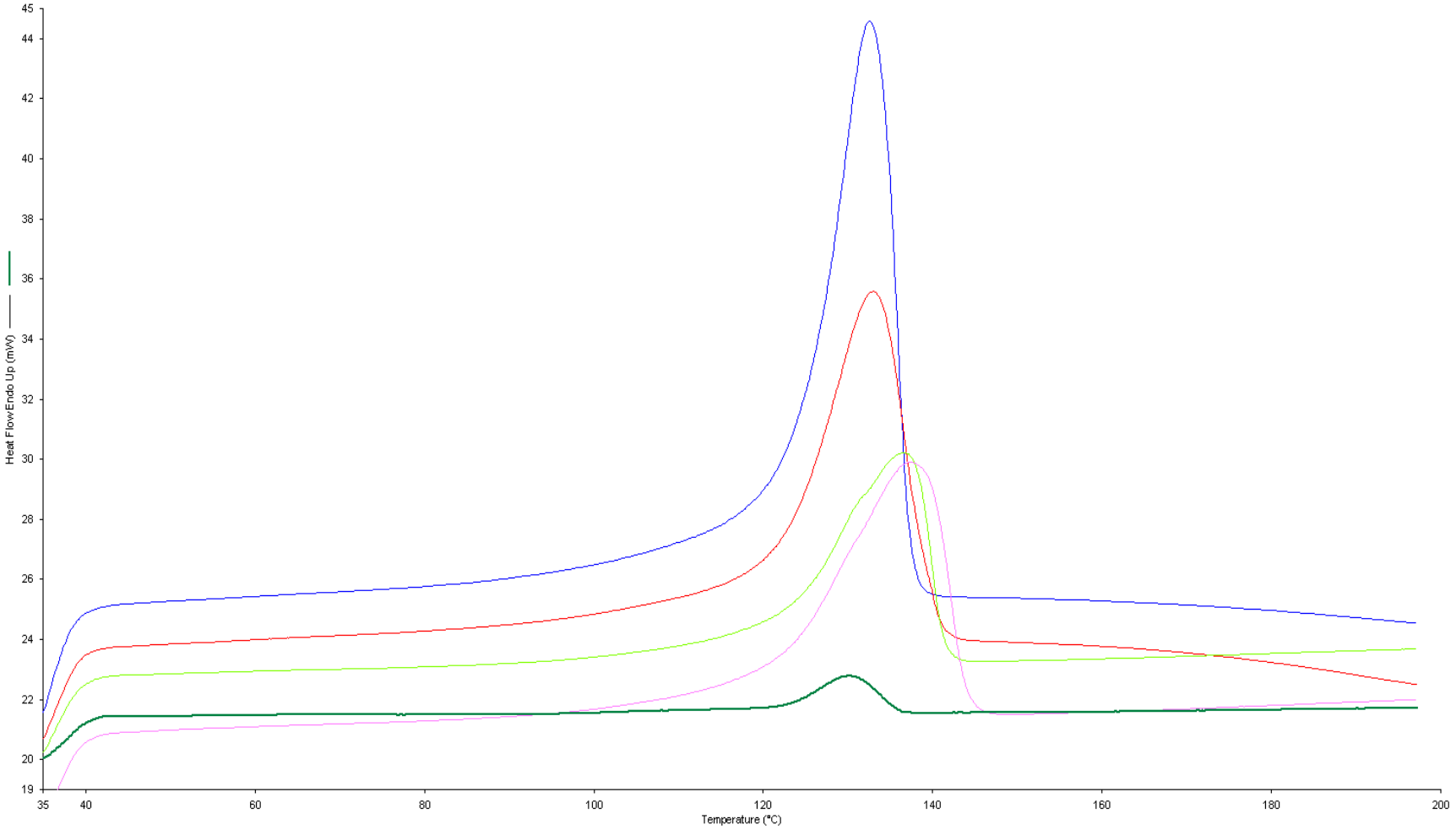

Figure 4.20: Effect of various Al / Cr ratios on the second DSC scan of polyethylene samples produced at Al / Cr ratio = 20, 35, 50, 45 and 30 respectively; $P_i \approx$ 855 kPa from bottom to the top using $[Cr_3O(F_3CCO_2)_6.3H_2O]NO_3.H_2O$ / $AlEt_2Cl$ catalytic system reaction, at T = 40 ^oC and 60 min reaction time

Table 4.9: DSC data for HDPE samples obtained using $[Cr_3O(F_3CCO_2)_6.3H_2O]NO_3.H_2O$ / $AlEt_2Cl$ catalytic system at different Al / Cr ratios and variable initial monomer pressures.

Cr:Al ratio	P_i (kPa)	1st scan			Cooling (crystallization)		2nd scan			Xc (%)
		T_m (^oC)	T_o (^oC)	ΔH (J/g)	T_c (^oC)	- ΔH (J/g)	T_m (^oC)	T_o (^oC)	ΔH (J/g)	
Series H										
1 :20	440	128.84	123.39	32.43	117.45	28.20	130.05	123..53	30.0	10.38
1 :20	530	131.52	123.30	100.69	116.11	69.71	130.55	122.73	83.06	28.74
1 :20	667	133.82	122.83	176.18	116.0	107.0	130.20	122.26	150.52	52.08
1 :20	865	138.58	129.48	152.58	113.71	118.52	133.15	120.63	118.07	40.85
1 :20	941	137.23	128.69	158.40	115.22	129.47	135.64	123.66	136.10	47.09
Series G										
1 :30	384	137.93	128.28	195.37	116.53	150.55	130.67	121.82	147.0	50.87
1 :30	500	143.23	124.94	150.94	116.32	133.21	131.50	123.11	133.12	46.06
1 :30	730	143.15	131.97	157.60	116.57	134.09	131.55	121.88	136.12	47.10
1 :30	825	145.0	125.65	164.20	113.70	151.60	133.7	121.69	163.71	56.65
1 :30	855	145.5	132.05	231.28	116.0	205.72	133.9	123.37	232.57	80.47
1 :30	913	145.92	125.0	160.80	117.63	146.66	134.27	119.76	164.54	56.93
Series I										
1 :35	529	142.39	130.0	185.98	114.34	153.34	133.10	121.0	169.76	58.74
1 :35	689	145.03	131.84	170.84	115.01	146.88	133.58	123.06	152.81	52.88
1 :35	844	147.07	134.63	231.34	114.86	198.81	134.24	123.77	210.83	72.95
1 :35	863	144.0	132.08	187.36	112.78	144.34	134.94	121.30	145.98	50.51
1 :35	947	141.57	130.26	154.34	114.88	126.66	135.65	119.87	133.48	46.19

Table 4.9: DSC data for HDPE samples obtained using $[Cr_3O(F_3CCO_2)_6.3H_2O]NO_3.H_2O$ / $AlEt_2Cl$ catalytic system at different Al / Cr ratios and variable initial monomer pressure. (continued)

Cr:Al ratio	P_i (kPa)	1st scan			Cooling (crystallization)		2nd scan			Xc (%)
		T_m (^oC)	T_o (^oC)	ΔH (J/g)	T_c (^oC)	- ΔH (J/g)	T_m (^oC)	T_o (^oC)	ΔH (J/g)	
Series J										
1 :45	342	141.04	128.0	167.89	114.43	121.58	135.44	122.22	124.67	43.14
1 :45	675	144.60	131.13	252.67	113.67	177.91	136.70	122.0	189.34	65.52
1 :45	822	139.24	121.09	252.21	113.37	250.33	138.15	122.40	223.15	77.21
1 :45	931	145.16	126.35	158.39	113.31	124.44	138.40	123.84	129.38	44.77
1 :45	1320	145.34	124.72	175.67	119.94	141.96	139.40	123.65	148.98	51.55
Series K										
1 :50	93	131.38	121.74	223.61	115.47	250.79	131.56	121.65	222.0	76.82
1 :50	286	141.43	121.57	229.03	114.27	205.59	136.79	121.75	210.30	72.77
1 :50	445	144.76	130.17	226.45	114.21	186.56	137.32	120.52	194.24	67.21
1 :50	869	144.32	124.36	189.88	113.17	154.69	138.70	123.82	158.24	54.75
1 :50	1083	143.26	128.21	187.41	114.23	115.45	139.33	126.81	164.76	57.01

Table 4.10: DSC data for HDPE samples obtained at variable Al / Cr ratios and similar initial monomer pressure.

Al / Cr ratio	P_i (kPa)	T_m (^oC)	T_c (^oC)	X_c (%)
20	865	133.15	113.71	40.85
30	855	133.9	116.0	80.47
35	863	134.94	112.78	50.51
45	822	138.15	113.37	77.21
50	869	138.70	113.17	54.75

4.5.5 Hardness

Hardness is an unusual physical property. In addition, its lack of a fundamental definition indicates that it is not a basic property of a material. It is well known in characterizing metallic material and ceramics for many years, but only recently, it has been widely used in the characterization of polymers. For elastomers and some polymers, hardness is defined as the resistance to elastic deformation on the surface of the material. Thus the higher the hardness of a polymer, the stronger the material is.

Prior to hardness measurements, samples were hot pressed and allowed to cool at ambient temperature. Each sample was measured at least five times, in different areas and the average value was considered as the hardness indicator. Table 4.11 and Table 4.12 summarize the data obtained respectively from PE, prepared at different initial monomer pressures and variable Al / Cr ratios.

The hardness values of the prepared polyethylene are in the range of 43.4 – 61.9 Shore D. As expected the higher values of hardness of the polyethylene surface correlate well with the higher crystallinity of the polymers.

Table 4.11: Hardness data of HDPE samples obtained at constant Al / Cr ratio and variable initial monomer pressures.

Al / Cr ratio	P_i (kPa)	T_m (^oC)	X_c^1 (%)	Hardness (Shore D)
30	500	131.50	46.06	50.3
30	730	131.55	47.10	52.8
30	825	133.70	56.65	55.3
30	855	133.90	80.47	61.9
30	913	134.27	56.94	55.5

X_c^1 is the crystallinity estimated from the DSC data

Table 4.12: Hardness data of HDPE samples prepared at variable Al / Cr ratios and similar initial monomer pressure.

Al / Cr ratio	P_i (kPa)	T_m (^oC)	X_c^1 (%)	Hardness (Shore D)
20	865	133.15	40.85	43.4
30	855	133.9	80.47	61.9
35	863	134.94	50.51	52.9
45	822	138.15	77.21	60.1
50	869	138.70	54.75	53.5

X_c^1 is the crystallinity estimated from the DSC data

4.5.6 Density

The density (ρ) of polyethylene is a measure of the proportion of crystals within its mass. Crystals, a result of the layering and close packing of polyethylene molecules, are denser than the tangled, disordered arrangement of molecules in the amorphous regions. Knowing the density for a polyethylene sample, its percentage of crystallinity (W_c), can be calculated using equation (1) [26, 27]:

$$W_c = \frac{\rho_a - \rho}{\rho_a - \rho_c} \quad (1)$$

Where

ρ_a = 0.854 g/cm^3 is the value of density of the amorphous phase

ρ_c = 0.997 g/cm^3 is the value of density of the crystalline phase

ρ is the average experimental value of density of the polymer sample

The density data from a series of experiments, carried out at constant Al / Cr and variable initial monomer pressures, are summarized in Table 4.13. Clearly the densities increase with the increase of hardness and crystallinity. However, it is important to point out that the degrees of crystallinity calculated from the density are slightly higher than those estimated from DSC results. This may be due to the fact that the powdered PE samples were hot pressed at 5 ^{o}C above their melting temperature followed by cooling at room temperature for 24 hours prior to determining the density measurements. Thus, the annealing process allows the polyethylene chains to realign correctly as required for an ordered crystalline structure and higher density was obtained after cooling. Similar observations are made for samples prepared with similar initial monomer pressure but variable Al / Cr ratios.

Table 4.13: Density data and comparison of degree of crystallinity obtained from DSC and density results

Al / Cr ratio	P_i (kPa)	T_m (^oC)	Hardness (Shore D)	ρ ($g.cm^{-3}$)	X_c^1 (%)	W_c^2 (%)
30	500	131.50	50.3	0.9247	46.06	49.4
30	730	131.55	52.8	0.9360	47.10	57.4
30	825	133.70	55.3	0.9370	56.65	58.0
30	855	133.90	61.9	0.9470	80.47	65.1
30	913	134.27	55.5	0.9413	56.94	60.0

X_c^1 is the crystallinity estimated from the DSC data
W_c^2 is the crystallinity calculated with the density value according to equation (1)

4.5.7 Dynamic Mechanical Analysis (DMA)

The mechanical properties of polymers are more highly diverse than those of any other class of materials [28]. Polyethylenes like other polymers are viscoelastic materials and DMA is an excellent tool for characterizing their viscoelastic properties. This is because the DMA technique helps provide information about the polymer relaxation transitions.

In this study, transitions were detected through the temperature dependence of the loss tangent (tan δ) and the loss modulus (E"). The storage modulus (E'), stiffness, loss modulus (E"), loss tangent (tan δ) and complex viscosity data were obtained from the DMA analysis. The tests were run with oscillation frequency of 1 Hz at a heating rate of 3 ^oC/min, from -140 ^oC to 40 ^oC unless stated otherwise. The strain amplitude was 20 μm and liquid nitrogen was used to cool the sample.

When exploring polyethylene features in the solid state, three relaxations (γ, β, and α-transitions) are commonly seen in the DMA curves [29]. Despite the large amount of published work on the subject, there is no consensus about the assignment of these relaxation temperatures.

The γ-relaxation typically appears in the -150 ^{o}C to -120 ^{o}C temperature range [30, 31]. It is independent of the degree of branching and has been associated with small local short-range segmental motion of the amorphous PE as well as the reorientation of loose chain ends within the crystalline and amorphous fractions [32, 33]. Several molecular models have been proposed to explain the γ-transition. Willbourn [34] has proposed that this relaxation was related to the restricted motion of short segments in the amorphous phase, involving at least four methylene groups. This has resulted in the so called "crankshaft motion" theory proposed by Schatzki [35] and Boyer [36]. Further results confirmed the analysis and the crankshaft model is widely accepted nowadays [32, 33].

The β-relaxation temperature is usually located between -50 ^{o}C and room temperature. It is related to the toughness which is usually observed in branched samples, and its intensity has been seen to decrease with increase in crystallinity. However, it has also been observed [37] in high molecular weight linear polyethylene. The β-transition is often attributed to the side chains or pendant components moving in the non-crystalline phase, either in the interfacial or amorphous regions. Several interpretations have been suggested for this relaxation. However, there is no general agreement in the literature about its mechanism. Different reports have observed the β-process to be a result of the relaxation of chain units located in the interfacial component [31], motions of long branches [38], interlamellar shear [33, 39, 40], the glass transition of polyethylene [32, 37], even as the the primary glass transition. The

hypothesis that crystal-amorphous interfacial compartments are involved in the β-relaxation indicates the lamellar fold surface morphology must contribute, in some way to the process [33].

It has been reported [30, 31] that the α–relaxation of various grades of polyethylene occurs over a wide range of temperatures (30 to 120 ^{o}C). It is usually found in all samples containing a high degree of crystallinity and is considered connected to the lamellar thickness [37]. Some reports have suggested that this transition involves a complex process of molecular mobility within the crystalline phase [29, 32].

In this work, all these morphological issues have been used to study the influence of monomer pressure and Al / Cr ratio on the relaxations of the prepared polyethylene samples using the storage modulus (E'), stiffness, loss modulus (E"), damping factor (tan δ) and complex viscosity curves.

In thermoplastics such as polyethylene, the storage and loss moduli change with temperature as the molecular mobility is affected. The storage modulus of a polymer decreases rapidly whereas the loss modulus and tan δ reach a maximum when the polymer sample is heated up through the glass transition (T_g) region [41] It is well known that the mobility of the amorphous components causes the reduction in the storage modulus. However, the material exhibits useful solid-state properties before approaching its melting temperature [42, 43]

Figures 4.21 and 4.22 show respectively an overlay of the storage modulus and stiffness of a series of polyethylene synthesized at constant Al / Cr ratio 30 and variable initial monomer pressures. The reaction time was 60 min, reaction temperature 40 ^{o}C and the $[Cr_3O(F_3CCO_2)_6.3H_2O]NO_3.H_2O$ / $AlEt_2Cl$ catalytic system was used. Four

experiments were run from - 140 to 40 ^{o}C and the last one from - 140 ^{o}C to 120 ^{o}C in order to study the behavior of the PE sample at high temperature.

As one can notice, the dynamic storage modulus is approximately similar to the stiffness. They both decrease with increase in temperature. This behavior is typical of polymeric materials since the chain movement and relaxation times of the polymer are reduced at lower temperature [42]. The deformation behavior of these materials changes as the temperature approaches the glass transition of amorphous polyethylene (≈ -120 ^{o}C). It is believed that the degree of crystallinity of the polymer and the molecular weight of the chains are the two factors which compete to determine the order in this region. It can also be observed in these figures (Figures 4.21 and 4.22) that the storage modulus and stiffness of the samples decreases, especially at low temperature, with increase in the degree of crystallinity of the polymer. The interpretation given here is that the highly crystalline PE probably has a high molecular weight chain and a restriction of chain movement at low temperature.

Figures 4.23 and 4.24 show the effect of temperature and monomer pressure on the loss modulus and tan δ responses for the PE samples. The loss modulus is a measure of the energy absorbed due to a relaxation and it is useful to point out the mechanism of internal motions. In addition, the damping factor (tan δ) is the ratio of the loss modulus to the storage modulus. It may also be obtained as the ratio of the real part to the imaginary part of the complex viscosity. Furthermore, it provides information on the relative contributions of the elastic and viscous components of a viscoelastic material.

For the temperature range studied, some PE samples exhibited the characteristic of γ (- 122 to -119 ^{o}C), β (- 54 to -41 ^{o}C), and α (above 50 ^{o}C), transitions from the loss and tan delta curves, whereas others present only the γ and α relaxations. As reported

above, the β-transition, which is often associated with the glass transition temperature of the amorphous polymer, is due to the motion of the branched segments of the chains. Therefore, it is seldom seen in linear polyethylene. However, it has been reported that the β-relaxation in linear polyethylene is only seen when the distance between the lamellae exceeds a certain value [44]. Also, it was attributed to the movement of free loops in the inter-lamellar space [45]. Comparing the tan delta responses of all PE samples during the γ-transition, the tan delta values reach a maximum value between (- 122 to -119 ^{o}C). It emerges that the magnitude of this transition depends on the degree of crystallinity of the polyethylene. The value of γ-relaxation is high for samples with a high degree of crystallinity. In addition, there is no appearance of β-relaxation at a high degree of crystallinity. The amount of branched chain is very limited in highly crystalline PE. After the β-transition, the α-relaxation occurs above 50 ^{o}C as the main chain motion within the crystalline phase begins.

Another important parameter to characterize the mechanical properties of polymer material is the complex viscosity (M_u*). Its data can be obtained from DMA analysis by the relation $M_u^* = E^* / 2(1 + \nu)$, where E^* is the complex modulus, $E^* = E' + iE''$ (E' is the storage modulus and E" the loss modulus), and ν is the Poisson ratio. In these experiments, the constant Poisson ratio of the instrument is 0.44. Figure 4.25 shows the complex viscosity versus temperature. The curves present a trend similar to those of storage modulus and stiffness. In addition, the PE samples show high viscosity and the complex viscosity decreases along with the increase in the degree of crystallinity.

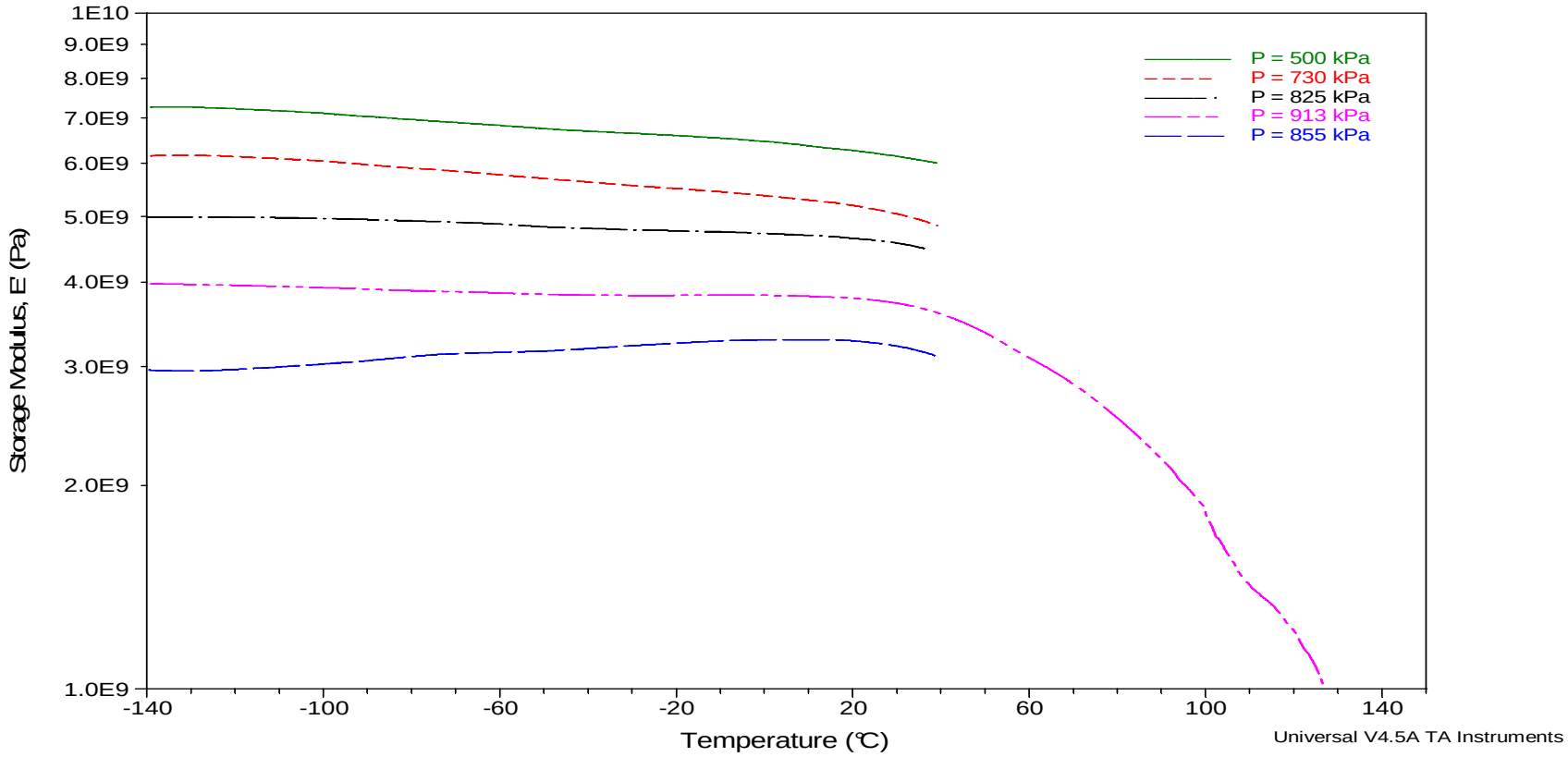

Figure 4.21: Effect of temperature on the storage modulus of PE with various initial monomer pressures, Al / Cr ratio of 30, reaction time = 60 min, T = 40 ^{o}C, catalytic system: $[Cr_3O(F_3CCO_2)_6.3H_2O]NO_3.H_2O$ / $AlEt_2Cl$

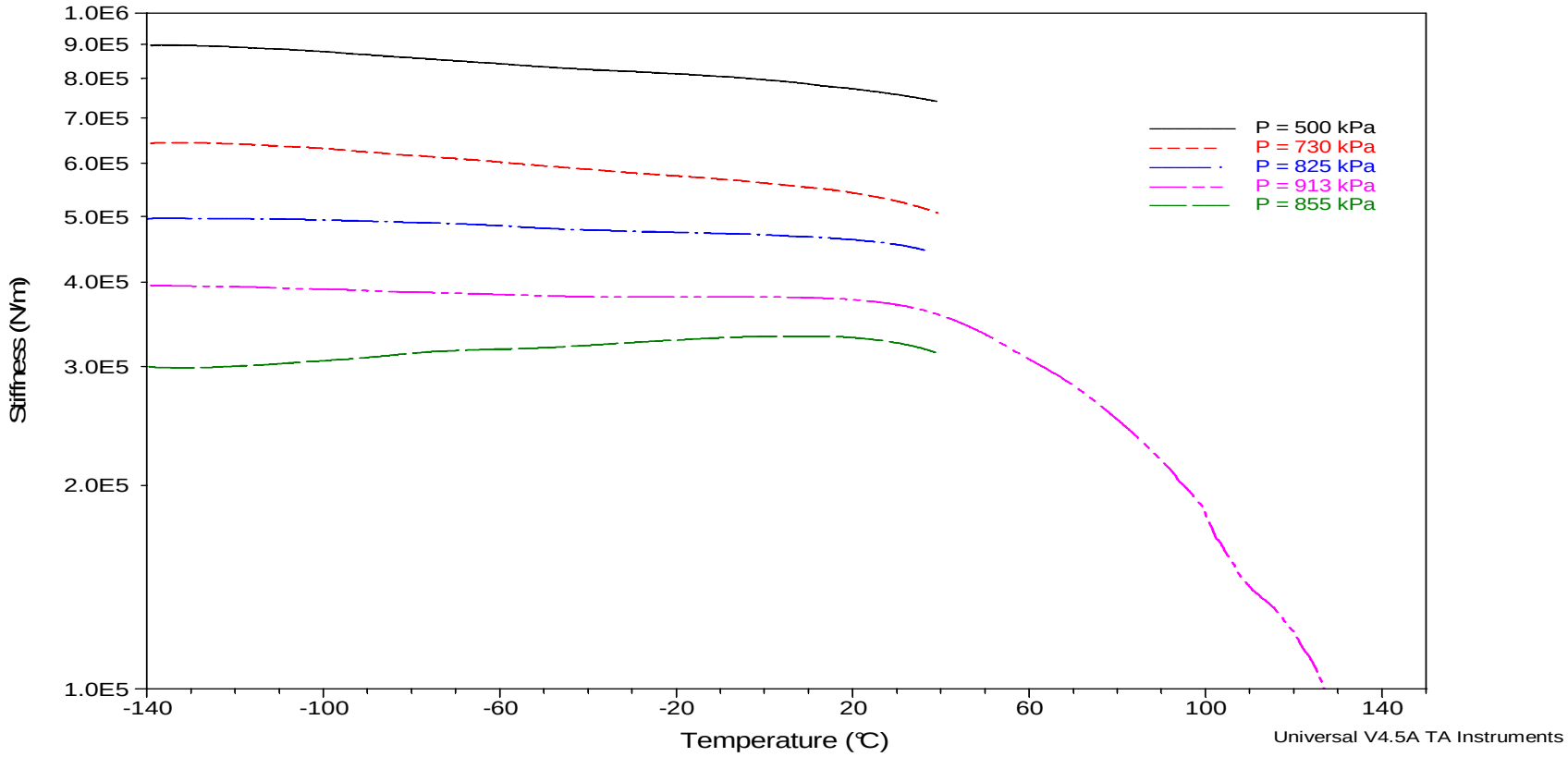

Figure 4.22: Effect of temperature on the stiffness of PE with various initial monomer pressures, Al / Cr ratio = 30, reaction time = 60 min, T = 40 ^{o}C catalytic system: $[Cr_3O(F_3CCO_2)_6.3H_2O]NO_3.H_2O$ / $AlEt_2Cl$

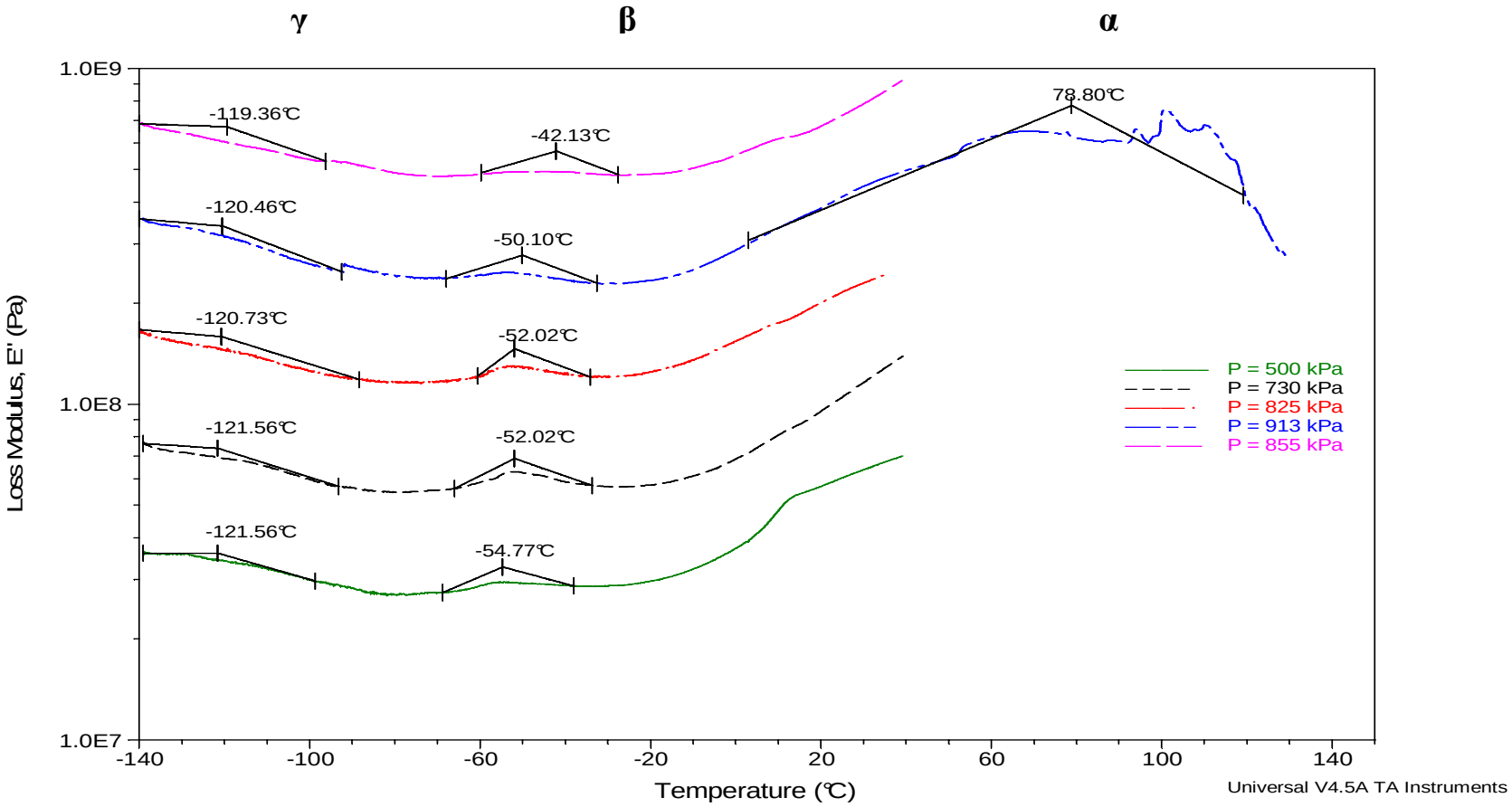

Figure 4.23: Effect of temperature on the loss modulus of PE with various initial monomer pressures, Al / Cr ratio = 30, reaction time = 60 min, T = 40 ^{o}C catalytic system: $[Cr_3O(F_3CCO_2)_6.3H_2O]NO_3.H_2O$ / $AlEt_2Cl$

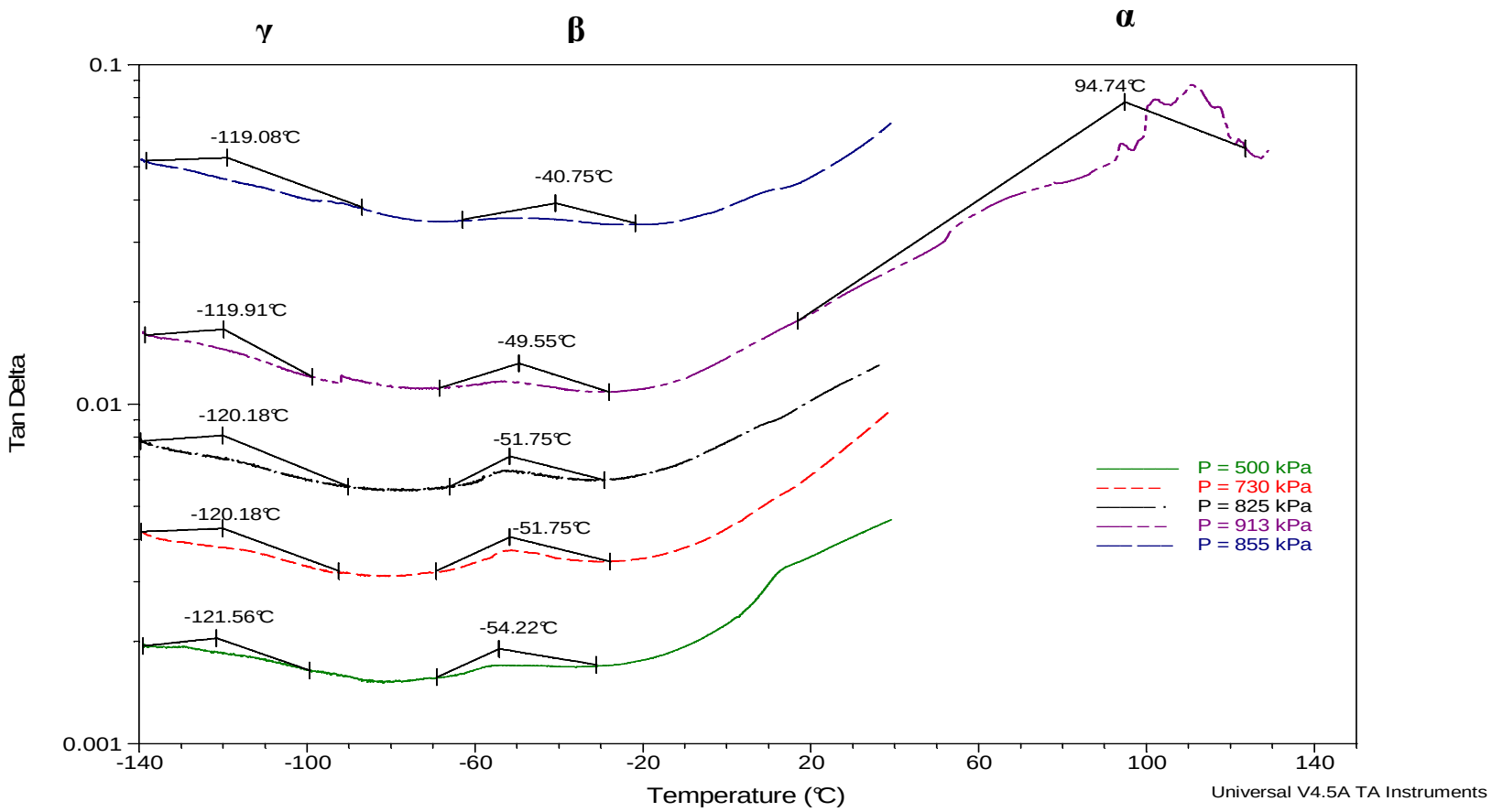

Figure 4.24: Effect of temperature on the Tan Delta of PE with various initial monomer pressure, Al / Cr ratio = 30, reaction time = 60 min, T = 40 ^{o}C catalytic system: $[Cr_3O(F_3CCO_2)_6.3H_2O]NO_3.H_2O$ / $AlEt_2Cl$

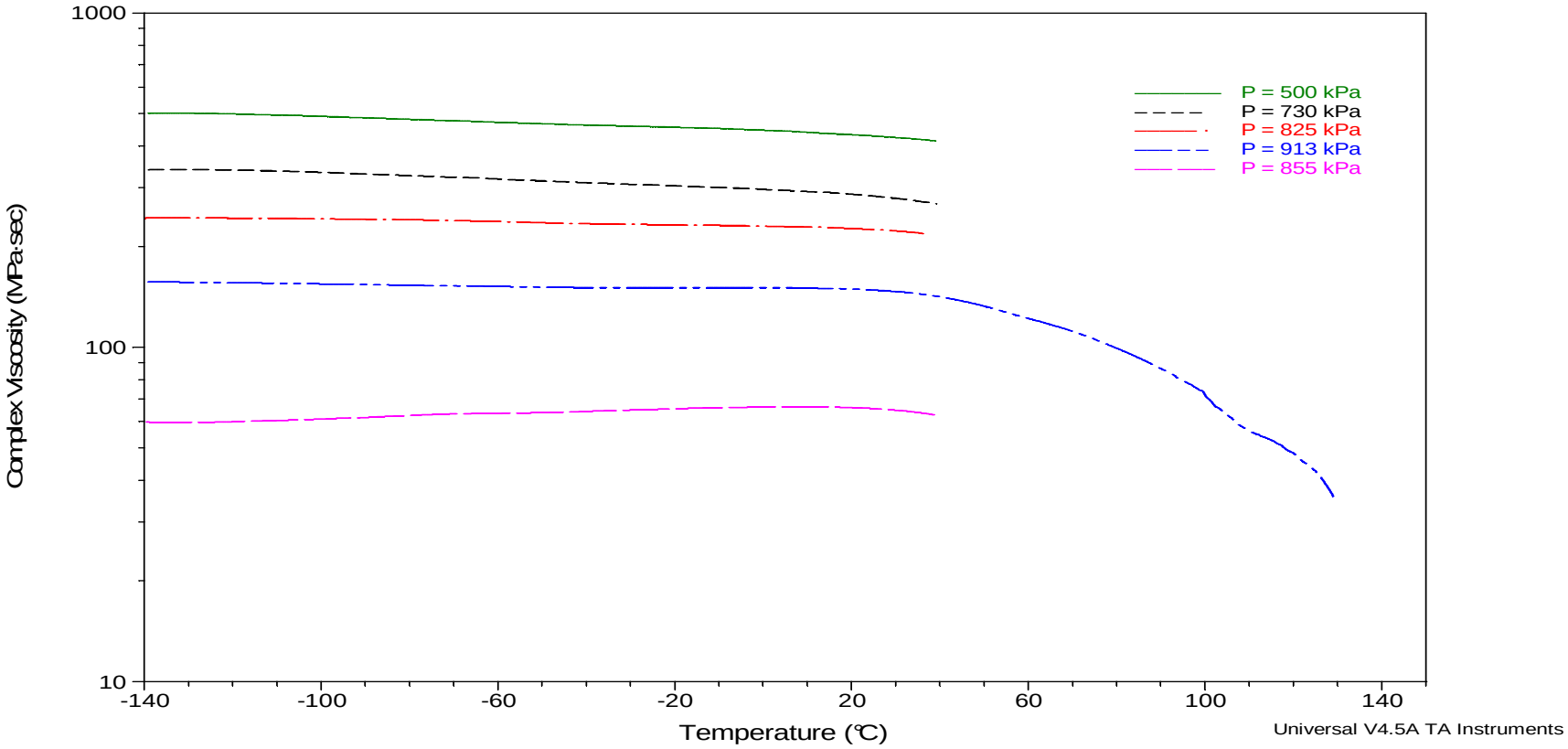

Figure 4.25: Effect of temperature on the complex viscosity of PE with various initial monomer pressures, Al / Cr ratio = 30, reaction time = 60 min, T = 40 ^{o}C, catalytic system: $[Cr_3O(F_3CCO_2)_6.3H_2O]NO_3.H_2O$ / $AlEt_2Cl$

The dynamic mechanical analyses of samples, with constant initial monomer pressure and variable Al / Cr, shows similar observations to those above described. Therefore, it can be concluded that there is no significant effect of pressure and Al / Cr ratio on the DMA results for PE. The only factors affecting the mechanical analysis are the degree of crystallinity and probably the molecular weight of the polymer.

4.5.8 Nuclear magnetic resonance spectroscopy (NMR)

From the above analyses, it is known that reaction conditions, such as Al / Cr ratio and ethylene pressure, strongly affect the structure of the PE obtained with the $[Cr_3O(F_3CCO_2)_6.3H_2O]NO_3.H_2O$ / $AlEt_2Cl$ catalytic system. NMR spectroscopy was used to probe the microstructure of the PE produced. The method used has been described in details in Chapter III.

It was very difficult to obtain the NMR data from these samples. Prior to the NMR analyses, they had to be heated in an oven for up to two hours at 140 ^oC in order to get the PE melted into solution. Both of ^1H NMR and ^{13}C NMR spectra were obtained.

High temperature (140 ^oC) ^1H NMR and ^{13}C NMR spectra of most of the polyethylene samples closely resembled those of ultra high molecular weight polyethylene (UHMWPE) [46], (Figures 4.26 and 4.27). Their ^1H NMR and ^{13}C NMR spectra have single peaks at around 1.5 ppm and 30.0 ppm, respectively. It has been reported that, because the molecular weight of this type of polyethylene samples are very high ($> 10^6$), only the main-chain carbon atoms are visible under normal spectral acquisition conditions [46, 47]. These ^1H NMR and ^{13}C NMR spectra were observed in highly crystalline samples which had their average melting temperature around 135 ^oC and did not show any β-transition in the DMA analysis.

Other types ^{1}H NMR and ^{13}C NMR spectra were obtained with lower degree of crystallinity samples produced at variable monomer pressures or various Al / Cr. A representative of each spectrum is shown in Figures 4.28 and 4.29. As one can see, there are two and four peaks in the ^{1}H NMR and ^{13}C NMR spectra respectively. This is typical of high density polyethylene (HDPE). Kaji et al. [46] and Brandolini et al. [47] demonstrated that linear polyethylene (HDPE) does have some branching. Even though HDPE is less branched than low density polyethylene (LDPE) and linear low density polyethyelene (LLDPE), ^{1}H NMR and ^{13}C NMR studies have shown respectively two and four peaks as shown below [47].

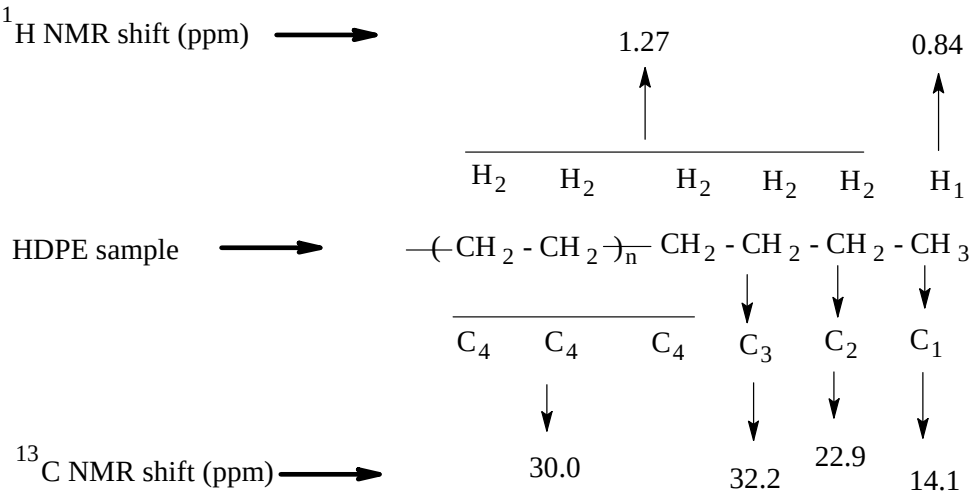

The presence of these branching peaks in the ^{13}C NMR spectra confirms the β-transition observed in the DMA curves for some PE samples. Therefore, it can be concluded that the degree of crystallinity also has a high impact on the NMR spectroscopy of the produced polyethylene.

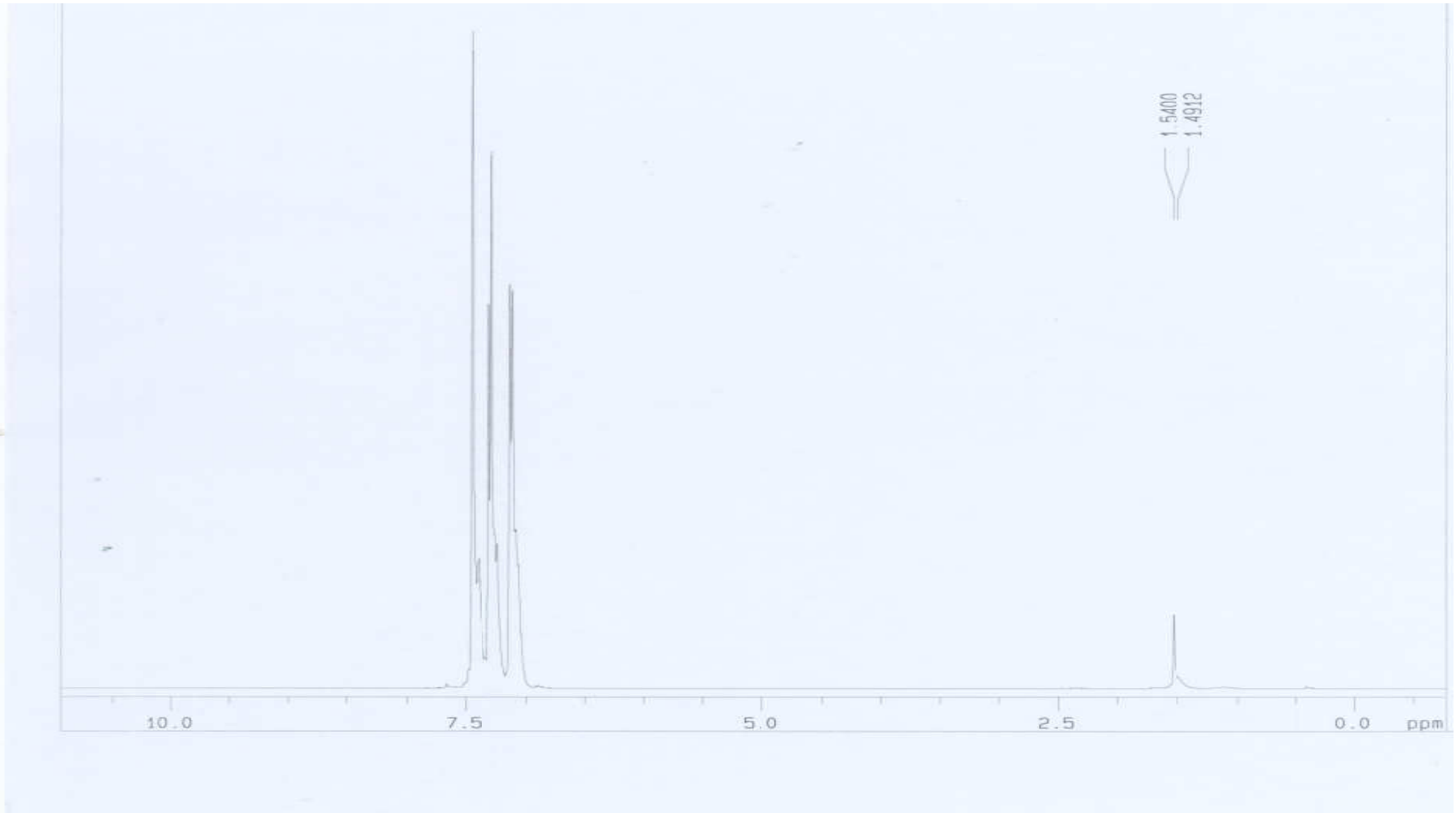

Figure 4.26: ^{1}H- NMR spectrum obtained from highly crystalline PE samples, produced at 40^{o}C, stirrer speed of 300 rpm in 60 min reaction time using $[Cr_3O(F_3CCO_2)_6.3H_2O]NO_3.H_2O$ / $AlEt_2Cl$ catalytic system

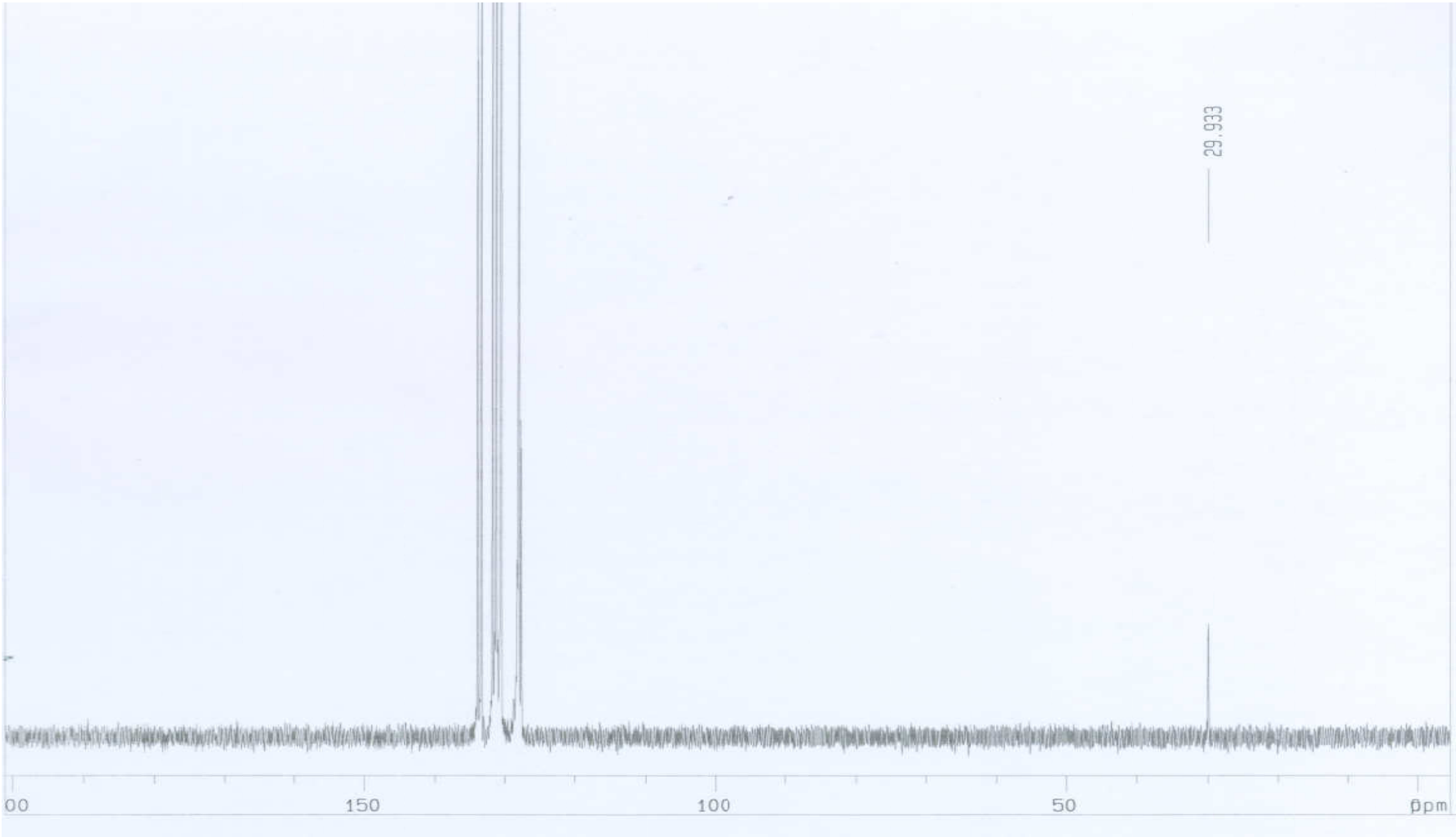

Figure 4.27: ^{13}C- NMR spectrum obtained from highly crystalline PE samples, produced at 40^{o}C, stirrer speed of 300 rpm in 60 min reaction time using $[Cr_3O(F_3CCO_2)_6.3H_2O]NO_3.H_2O$ / $AlEt_2Cl$ catalytic system

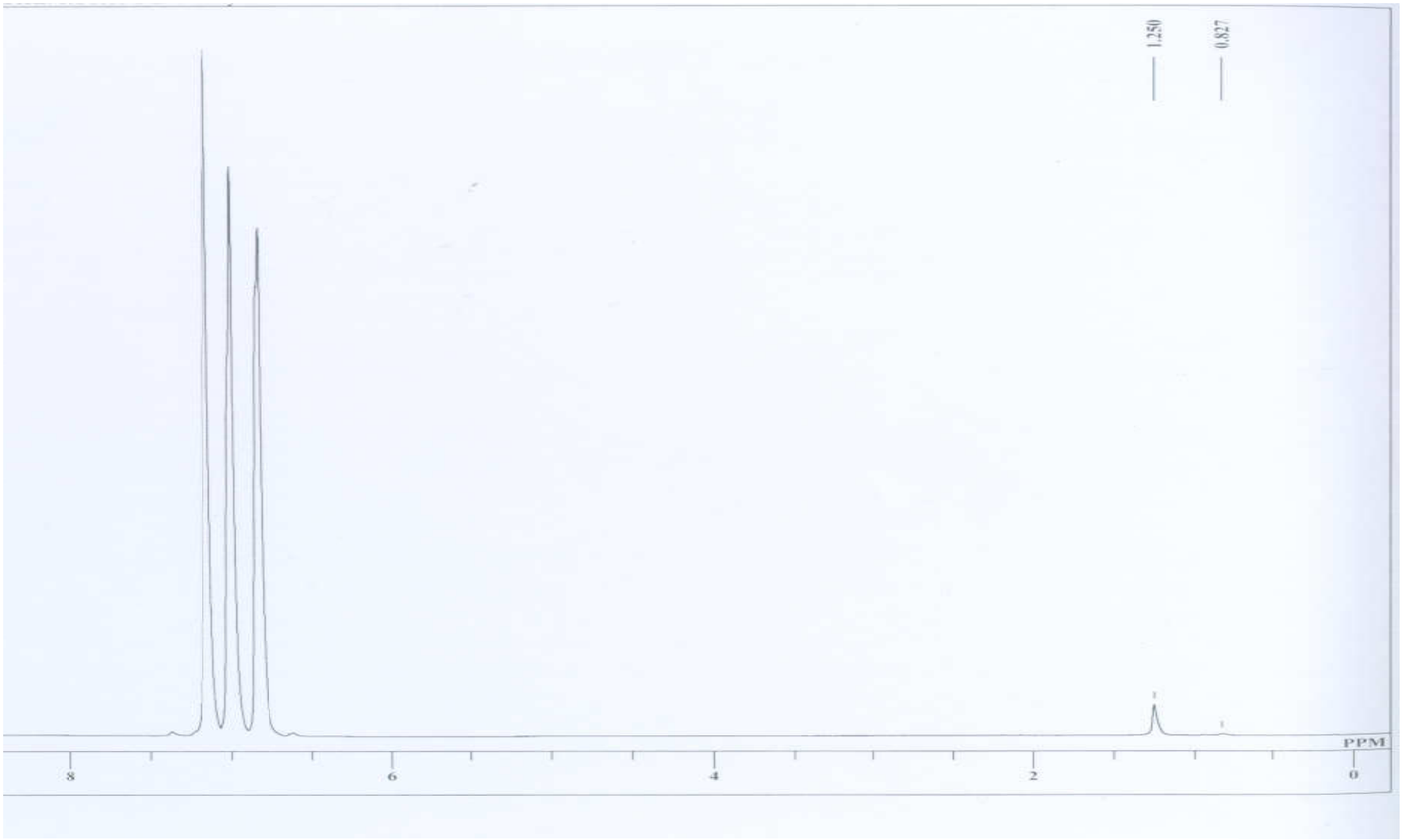

Figure 4.28: Second type of ^{1}H- NMR spectrum obtained from PE samples, produced at 40^{o}C, stirrer speed of 300 rpm in 60 min reaction time using $[Cr_3O(F_3CCO_2)_6.3H_2O]NO_3.H_2O$ / $AlEt_2Cl$ catalytic system

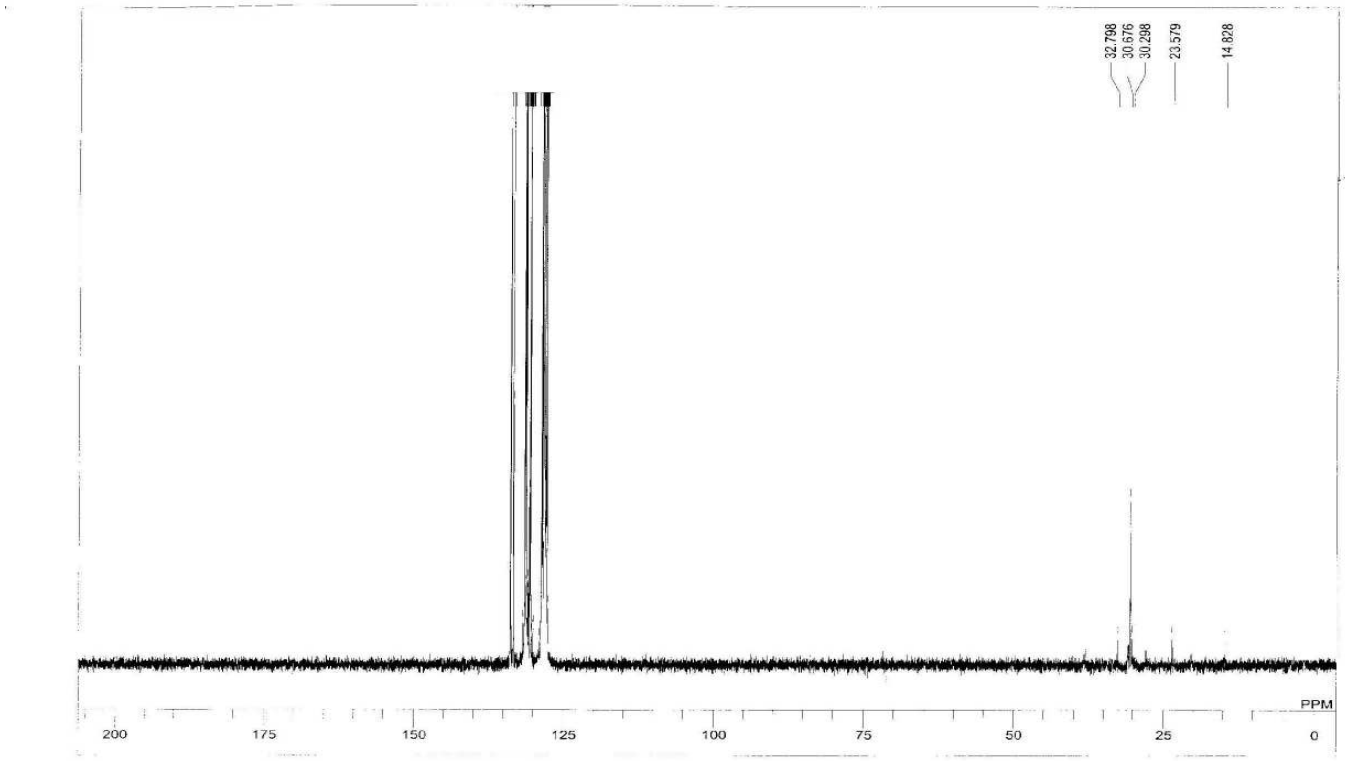

Figure 4.29: Second type of ^{13}C- NMR spectrum obtained from PE samples, produced at 40^{o}C, stirrer speed of 300 rpm in 60 minutes reaction time using $[Cr_3O(F_3CCO_2)_6.3H_2O]NO_3.H_2O$ / $AlEt_2Cl$ catalytic system

4.6 Conclusion

The system $[Cr_3O(F_3CCO_2)_6.3H_2O]NO_3.H_2O$ / $AlEt_2Cl$ has been investigated as a potential heterogeneous Ziegler-Natta catalyst for the homopolymerization of ethylene. The catalyst was found to be highly active. Maximum activity (13.9 kg-PE/g-Cr/hr/atm) was obtained at Al / Cr molar ratio of 45 and initial monomer pressure of 1320 kPa. The Al / Cr ratio and ethylene pressure were found to affect the rate of the polymerization. Maximum rate was obtained at high monomer pressure or with increased Al / Cr ratio.

The kinetic data for the polymerization showed a first order reaction at the beginning. Activity decreased very rapidly because of the deactivation of active centers.

The FTIR, DSC, hardness, density, DMA and NMR analyses showed that the polymerization of ethylene, using the $[Cr_3O(F_3CCO_2)_6.3H_2O]NO_3.H_2O$ / $AlEt_2Cl$ catalytic system, is affected by the monomer pressure and the Al / Cr molar ratio. The polymers produced are highly crystalline polyethylene.

4.7 References

1. S. N. Gan, S. I. Chen, R. Ohnishi and K. Soga, Makromol. Chem. Rapid. Commun., **5**, 535 (1984).
2. S. N. Gan, M. C. Lim, S. I. Chen and K. Soga, J. Catal., **105**, 249 (1987).
3. K. Soga, S. I. Chen, T. Shiono and Y. Doi, Polymer, **26**, 1888 (1985).
4. G. M. Burnett and P. J. T. Tait, Polymer, **1**, 151 (1960).
5. A. Schindler, Polymer Letters, **3**, 793-795 (1965).

6. V. A. Zakkarov, G. D. Bukatov and Y. I. Ermakov, Adv. Polym, **18**, 179 (1977).
7. C. P. Ooi, Master thesis, University of Malaya, Kuala Lumpur, 1996.
8. S. M. Nelana, J. Darkwa, I. A. Guzei and S. F. Mapolie, J. Org. Chem., **689**, 1835-1842 (2004).
9. F. F. N. Escher, R. S. Mauler and R. F. de Souza, J. Braz. Chem. Soc., **12** (1), 47-51 (2001).
10. J. Boor Jr., Ziegler-Natta Polymerization and Catalysts, Academic Press, New York, (1972).
11. T. Keii, K. Soga, S. Go, A. Takahashi, A. Kohima, J. Polym. Sci.(C), 23, 453 (1968).
12. U. Giannini, Makromol. Chem. Suppl., **5**, 216-229 (1981).
13. A. Munz-Escalona and J. Villalba, Polymer, **18**, 179 (1977).
14. H. Mori, K. Ohnishi and M. Terano, Macromol. Rapid Commun., **17**, 25-29 (1996).
15. S. N. Gan, S. I. Chen, R. Ohnishi and K. Soga, Polymer, 28, 1391 (1987).
16. H. Schnecko, M. Reinmoller, K. Weirauch and W. Kern, J. Polym. Sci. (C), **4**,71 (1964).
17. Goliath Business News, "Identification of polymers by IR spectroscopy", (2004). http://goliath.ecnext.com/coms2/gi_0199-498093/Identification-of-polymers-by-IR.html
18. Sutherland, Discuss. Faraday Soc., **9**, 274 (1950).
19. Sheppard and Simpson, Quarterly Reviews, **7**, 19 (1953).
20. L. J. Bellamy, "The IR Spectra of Complex Molecules, J. Wiley & Sons, New York, 18 (1959).
21. Sheppard and Sutherland, Nature, **159**, 739 (1947).

22. F. M. Mirabella, Simultaneous DSC and IR Spectroscopy, Am. Chem. Soc., Washington D. C. (1990).
23. L. H. Sperling, “Introduction to Physical Polymer Science”, J. Wiley & sons., Inc. 328 (1992).
24. X. Xu, J. Xu, K. Feng, W. Chen, J. Appl. Polym. Sci., **77**, 1709-1715 (2000).
25. A. M. Jelan. PhD thesis, University of Malaya, Kuala Lumpur, (1995).
26. A. Min Min, T. G. Chuah and T. R. Chantara, Material and Design, **29**, 992 – 999 (2008)
27. P. J. Sinko and A. N. Martin, “Martin's physical pharmacy and pharmaceutical sciences”, 5th edition, 606 – 607 (2005).
28. A. V. Tobolsky, Properties and structures of Polymers, J. Willey & Sons, Inc., New York (1960).
29. A. Pegoretti, M. Ashkar, C. Migliaresi, G. Marom, Comos. Sci. Technol., **60**, 1181 – 1189 (2000).
30. N. Alberola, J. Y. Cavaille and J. Perez, J. Polym., Sci. (B), Polym Phys. Ed., **28**, 569 (1990).
31. R. Popli, M. Glotin, L. Manderlkern, J. Polym. Sci. Polym. Phys. Ed., **22**, 407 (1984).
32. R. H. Boyd, Polymer, **26**, 1123 (1985).
33. R. O. Sirotkin and N. W. Brooks, Polymer, **42**, 9801 (2001).
34. A. H. Willbourne, Trans. Faraday Soc., **54**, 717 (1958).
35. T. F. Schatzki, J. Polym. Sci. **57**, 337 (1962).
36. R. F. Boyer, Rubber Chem. Technol., **34**, 01303 (1963).
37. K-h. Nitta and A. Tanaka, Polymer, **42**, 1219-1226 (2001).
38. J. V. Gulmine and L. Akcelrud, Eur. Polym. J., **42,** 553 (2006).
39. Z. H. Stachurski and I. M. Ward, J. Polym. Sci., **6**, 1817 (1968).

40. Z. H. Stachurski and I. M. Ward, Macromol Sci B3, **3**, 445 (1969).

41. S. Yang, J. Taha-Tijerina, V. Serrato-Diaz, K. Hernandez and K. Lozano, Composites, Part B, **38**, 228 – 235 (2007).

42. K. Menard, Dynamic Mechanical Analysis: a practical introduction, CRC Press LLC, USA, (1999).

43. M. Sepe, "Dynamic Mechanical Analysis for plastics engineering", Plastics Design Library, USA, (1998).

44. A. G. Simanke, G. B. Galland, L. Freitas, J. A. H. da Jornada, R. Quijada and R. S. Mauler, Polymer, **40**, 5489-5495 (1999).

45. S. Bensason, J. Minick, A. Moet, S. Chum, A. Hiltner and E. Baer, J. Polym. Sci., Part B, Polym. Phys., **34**, 1301-1315 (1996).

46. A. Kaji, Y. Akimoto and M. Murano, J. Polym. Sci. (A) Polym. Chem., 29, 1987 (1991).

47. A. J. Brandolini, D. D. Hills, "NMR Spectra of Polymers and Polymer Additives" New York, Marcel Dekker, (2000).